 doi:10.20944/preprints202205.0184.v1

Article

Amyloid Precursor Protein, Alpha-, Beta- and Gamma-Secretases Expression in Penumbra Cells after Photothrombotic Stroke. Evaluation of the Neuroprotective Effect of Secretase Inhibitors

Svetlana Sharifulina [a], Valeria Guzenko [a], Alexandr Logvinov [a], Andrey Khaitin [a], Yuliya Kalyuzhnaya [a], Natalia Dobaeva [b],Yan Li [c], Lei Chen [c], Bin He [c], Svetlana Demyanenko [a]

[a] Laboratory of Molecular Neurobiology, Academy of Biology and Biotechnology, Southern Federal University, pr. Stachki 194/1, Rostov-on-Don 344090, Russia.
[b] Department of General and Clinical Biochemistry no.2, Rostov State Medical University, st. Nakhichevansky 29, Rostov-on-Don 344000, Russia
[c] State Key Laboratory of Functions and Applications of Medicinal Plants; Engineering Research Center for the Development and Application of Ethnic Medicine and TCM (Ministry of Education); Guizhou Provincial Key Laboratory of Pharmaceutics; School of Pharmacy; School of Basic Medical Science; Guizhou Medical University, Guiyang 550004, China.
* Correspondence: svetlana.sharifulina@gmail.com

Abstract: Photothrombotic stroke (PTS) stimulates the level of N- and C-terminal fragments of Amyloid precursor protein (APP) growth in the cytoplasm of ischemic penumbra cells not earlier but at 24 hours. Here we have shown that APP fragments are visualized in thin unmyelinated fibers of neurons, in containing mitochondria large fibers and in synapses but absent in the nuclei. At 24 hours after PTS, some elements of the destroyed tissue accumulated a significant amount of APP protein. The level of ADAM10 α-secretase decreased on the first day after PTS in the rat brain cortex and ADAM-10 co-localized with the lipid raft marker caveolin-1. PTS caused no changes in the level of β-secretase BACE1 either on the first day after PTS or in the early recovery period. The expression of proteins of the γ-secretase complex: presenilin-1 and nicastrin increased in astrocytes, but not in penumbra neurons after PTS. The β-secretase inhibitor LY2886721 did not affect the infarct size of the mouse cerebral cortex and the level of apoptosis of cells in the perifocal region after PTS. Whereas the inhibitor of γ-secretase DAPT reduced the expression of glial fibrillary acidic protein (GFAP) in astrocytes, prevented the growth of apoptosis of mouse cerebral cortex cells reducing the infarct volume on the 7th and 14th days after PTS. DAPT may be considered as a drug for stroke therapy.

Keywords: amyloid precursor protein; photothrombotic stroke; ischemia; alpha-secretase; beta-secretase; gamma-secretase

1. Introduction

Stroke is the second leading cause of mortality and the major cause of adult physical disability worldwide [1]. Preclinical testing of hundreds of potential drugs did not determine the drugs without serious side effects that limit the spread of pathological processes from the primary site of damage to surrounding healthy tissues and protect nerve cells in them [2, 3]. Their search requires deep and comprehensive studies of the molecular mechanisms of neurodegeneration and neuroprotection in these pathological processes.

Our previous proteomic studies have shown that expression of APP, nicastrin and apolipoprotein E (APOER or LRP1) , which is involved in the processing and functioning of APP, increased in the penumbra at 1-4 hours after acute photothrombotic exposure. That is why we decided to study APP and its proteolytic system in stroke [4].

Preprints (www.preprints.org) | NOT PEER-REVIEWED | Posted: 13 May 2022 doi:10.20944/preprints202205.0184.v1

The APP protein (amyloid precursor protein) has been intensively studied since the 1980s due to its central role in the development of Alzheimer's disease (AD). Its fragment, β-amyloid peptide (Aβ), accumulating in amyloid plaques in the brain of patients, is one of the main pathogenesis of AD. APP plays an important role in various human and animal cells. It is an evolutionarily conserved protein [5, 6]. High level of APP expression in the brain indicates an important role in the nervous system. It is involved in processes of development, differentiation and function of neurons, in the growth of neurites, the formation of synapses and long-term memory, in the maintenance of brain integrity and in the reactions of neurons to damage [7, 8]. However, the specifically biochemical and physiological functions of APP and its proteolytic products are still unknown. The accumulation of APP in damaged neurons during ischemic exposure indicates its important role in the development of damage and neurodegeneration after stroke [9, 10].

APP is a large transmembrane glycoprotein that crosses the plasma membrane (PM) once. Its large N-terminal domain faces the extracellular environment, while its small C-terminal domain faces the cytoplasm. APP undergoes proteolytic cleavage by α-, β-, and γ-secretases to form a number of peptides: sAPPα (soluble amyloid precursor protein alpha), sAPPβ (soluble amyloid precursor protein beta), Aβ (β-amyloid peptide), AICD (amyloid precursor protein intracellular domain) and some less studied peptides. APP proteolytic products have independent activity and are involved in various cellular processes. There are amyloidogenic and non-amyloidogenic pathways of APP proteolysis (Fig. 1).

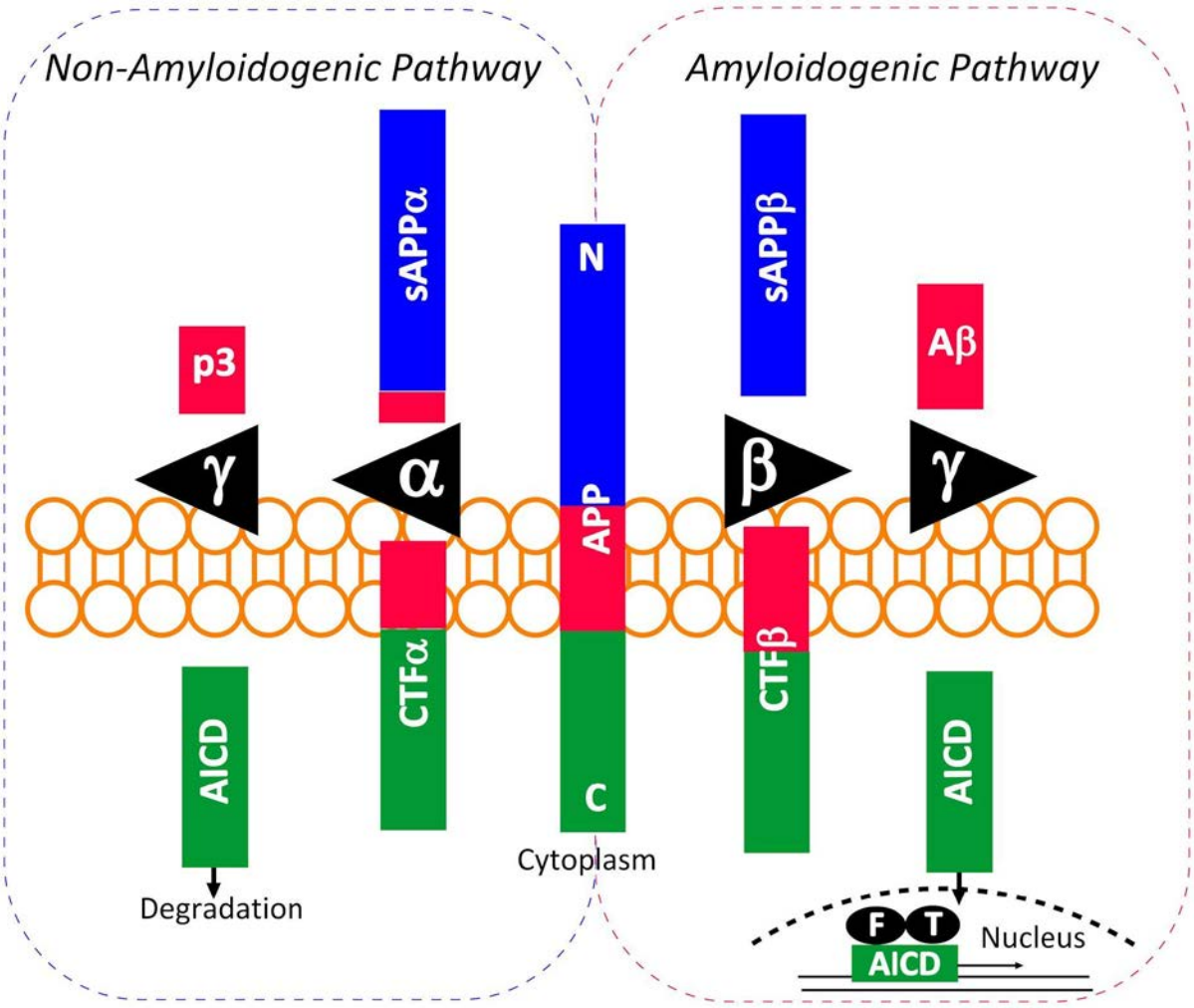

Figure 1. APP proteolysis and its enzymes. In the non-amyloidogenic pathway, α-secretase (α) cleaves APP in the Aβ region with the release of a soluble neuroprotective sAPPα fragment and a CTFα fragment into the medium, and then γ-

 doi:10.20944/preprints202205.0184.v1

secretase (γ) cleaves CTFα to p3 peptide and AICD, which passes into the cytoplasm, where it undergoes degradation. In the amyloidogenic pathway, β-secretase (β) cleaves the soluble sAPPβ fragment, and then γ-secretase (γ) cleaves the APP fragment remaining in the membrane (CTFβ), releasing the Aβ amyloid peptide into the cytoplasm and releasing the short AICD peptide into the cytoplasm, which is transferred with the help of the Fe65 (F) to the nucleus where in combination with the Tip60 (T) protein it plays the role of a transcription factor.

In the non-amyloidogenic pathway, α-secretase cleaves a large N-terminal fragment of sAPPα from APP. At the same time, Aβ, the APP fragment immersed in the membrane, is cleaved and inactivated. Then, γ-secretase built into the membrane cleaves off the intracellular AICD peptide, which is degraded in the cytoplasm. Cleavage of APP by α-secretase occurs mainly on the cell surface, although some part of APP is cleaved along the pathways of processing and traffic in cisterns and vesicles of the endoplasmic reticulum and Golgi apparatus [11, 12]. Proteinases of the ADAM (a disintegrin and metalloproteinase) family act as α-secretase in mammalian cells, and ADAM10 protein plays the main role in APP processing in the non-amyloidogenic pathway [13,14].

β-secretase is an aspartyl protease represented by two main isoforms BACE1 (beta-site APP cleaving enzyme 1) and BACE2. BACE1 is abundant in the nervous system, such as in neurons, astrocytes, and oligodendrocytes, while BACE2 is abundant in peripheral tissues, such as melanocytes or pancreatic β-cells. In the amyloidogenic pathway, BACE1 and γ-secretase cleave APP in the plasma membrane so that the Aβ peptide is released into the environment, and AICD is released into the cytoplasm. During cerebral ischemia, BACE1 is activated as a result of oxidative stress and stimulation of the oxygen sensor HIF1α [15, 16]. γ-secretase is a large multi-subunit enzyme consisting of presenilin-1 (PS-1), which actually performs a proteolytic function, presenilin-2 (presenilin enhancer 2, PEN2), associates and causes the endoproteolysis of PS into the N-terminal fragment (NTF) and C-terminal fragment (CTF), nicastrin (NCT), which is involved in substrate recognition, and the APH-1 (anterior pharynx-defective 1) protein, which forms a platform for subunit binding [17]. One of the results of γ-secretase activity are the release of the amyloid peptide Aβ into the extracellular environment, which stimulates the development of Alzheimer's disease, and the release of the rest part into the cytoplasm as the transcription factor AICD, which regulates the expression of a number of proapoptotic genes [11].

In this study we investigated the expression and localization of the APP protein in rat brain cells after photothrombotic stroke (PTS). We have studied the expression and localization of α-secretase ADAM10, β-secretase BACE1, and components of the γ-secretase complex presenilin 1 and nicastrin involved in APP proteolysis in rat brain neurons and glial cells after PTS. Also we have studied the effect of secretase inhibitors on apoptosis and volume of mouse brain infarction after PTS.

2. Methods

Antibodies

For Western blot analysis and immunofluorescence microscopy, rabbit antibodies were used: anti-ADAM-10, C-terminus (A2726); anti-BACE1 (SAB2100200); anti-nicastrin (ab1) (PRS3983); anti-presenilin-1 (PRS4203); mouse antibodies NeuN (marker of neurons) (MAB377), GFAP (marker of astrocytes) (SAB5201104) anti-caveolin-1 (marker of lipid raft) (SAB4200216). To determine the expression and localization of the APP protein by Western blot analysis and immunoelectron microscopy in nerve cells, we used antibodies that specifically recognize the N- or C-terminal fragments of the APP protein (N-APP and C-APP). According to the manufacturer (Sigma-Aldrich), the anti-rabbit N-APP antibody (SAB4200536) recognizes the N-terminal extracellular domain of human, rat or mouse APP and its proteolytic products sAPPα and sAPPβ. The anti-rabbit C-APP antibody (A8717) is specific for the sequence of amino acids 676-695 at the C-terminus of APP. It recognizes the C-terminus of the integral APP protein built into the membrane, as well as

 doi:10.20944/preprints202205.0184.v1

the AICD peptide. All antibodies and reagents used were purchased from the Moscow branch of Merck (Moscow, Russia).

Animals

The experiments were carried out on adult male rats (200-250 g). The experiments with HDAC inhibitors were performed on male mice of the outbred CD-1 stoke (14-15 weeks old, 20-25 g). Outbrand Wistar rats and CD-1 mice were purchased from a nursery in Pushchino, Moscow Region (http://www.spf-animals.ru/animals/rats/). Outbred white mice and rats are from the vivarium of the FBUN of the Rostov Research Institute of Microbiology and Parasitology. Animals were kept in standard cages in groups of 4–5 animals with free access to food and water. The animal housing was maintained under standard conditions: cycle 12 light/12 dark, 22-25°C, air exchange rate 18 shifts per hour. International, national and/or institutional guidelines for the care and use of animals have been followed. All experimental procedures were carried out in accordance with European Union directives 86/609/EEC on the use of experimental animals and local legislation on the ethics of animal experimentation. Animal protocols have been evaluated and approved by the Animal Care and Use Committee of the Southern Federal University (Permit No. 08/2016). Throughout the entire period of detention and before the experiment, the animals were properly cared for with daily veterinary examination (body position in space, activity), thermometry and weighing of each animal. Adequate depth of anesthesia was achieved in about 30 minutes. Depth of anesthesia was assessed by testing reflexes. Namely, the absence of a plantar reflex and a reaction to pinching the membrane between the fingers, and in addition, a decrease / absence of muscle tone in the limbs, a slow even rhythm of heart contractions and breathing. The following measures of physiological support of the animal during the state of anesthesia and experimental procedures were observed: prevention of dry eyes and damage to the cornea by placing an ophthalmic ointment in the conjunctival sac; temperature support provided by an electrically heated mat. After the surgical intervention, each animal was placed in a separate warm clean cage until complete recovery from anesthesia. Further postoperative care included the administration of analgesics, antimicrobials, daily monitoring of the condition of the animals for signs of pain and distress, special attention was paid to the condition of the sutures and the radiation area.

Photothrombotic stroke model

As a model of ischemic stroke, we used unilateral photothrombotic stroke (PTS) in the somatosensory cortex of the brain of rats or mice. In PTS, local laser irradiation induces photoexcitation of the introduced photosensitizing dye Bengal rose. Due to its physical properties, it does not penetrate the cells and remains in the blood vessels. After laser irradiation, highly reactive singlet oxygen is generated, which damages the vascular endothelium causing platelet aggregation and vascular thrombosis [18].

Experiments were done as described before [19]. Briefly, rats were anesthetized with intraperitoneal injections of telazol (50 mg/kg) and xylazine (10 mg/kg). The animals were fixed, the periosteum was removed, and a longitudinal incision was made in the skull skin. Rose Bengal (20 mg/kg) (R4507, Merck, Moscow, Russia) was injected into the subclavian vein. Then the somatosensory cortex (3 mm lateral to the bregma) was irradiated through the relatively transparent cranial bone with a diode laser (532 nm, 60 mW/cm^2, Ø3 mm, 30 min). This mode of exposure contributes to the formation of an infarct core with a diameter of about 3 mm, which is surrounded by a penumbra about 1.5 mm wide [19]. After anesthesia, the rats were decapitated at 4 hours, 24 hours, or 7 days after PTS. The brain was removed and a section of the cortex corresponding to the core of the infarction was removed on ice with a cylindrical knife Ø3mm, and then a 2-mm ring was cut around the irradiation zone with another knife Ø7mm, approximately corresponding to the penumbra tissue (experimental sample, respectively, PTS4, PTS24

 doi:10.20944/preprints202205.0184.v1

and PTS7d). The control groups included sham-operated (SO) animals subjected to the same operations, but without the introduction of a photosensitizer. The obtained tissue samples were further used for Western blot analysis.

Experiments with inhibitors of α-, β- and γ-secretases were carried out on mice. Mice were anesthetized at 25 mg/kg telazol and 5 mg/kg xylazine. Rose Bengal at a concentration of 15 mg/ml was administered intraperitoneally at a dose of 10 μl/g of body weight. At 5 minutes after the introduction of the photosensitizer, the area of the mouse skull, freed from the periosteum, in the region of the sensorimotor cortex (2 mm lateral to the bregma) was irradiated with a diode laser. Irradiation parameters: wavelength 532 nm, intensity 0.2 W/cm^2, beam diameter 1 mm, duration 15 min. The control groups included SO animals subjected to the same operations, but without the introduction of a photosensitizer. 3, 7, and 14 days after laser irradiation, the mice were decapitated, and the brain was removed to study the extent of damage, the level of apoptosis of cells in the perifocal region, and the expression of the GFAP protein in astrocytes. The surgery is non-invasive, with 100% survival of animals before the decapitation.

Immunoblotting

Expression of ADAM10, BACE1, presenilin 1, and nicastrin in the cytoplasmic fraction of rat cerebral cortex cells after PTS was studied using the Western blot method as described previously [20]. Briefly, animals were decapitated at 4 or 24 hours after PTS, the brain was removed, and the infarction area was cut out from the cortex on ice with a 3-mm cylindrical knife, and then a ring with a 2-mm splint corresponding to the penumbra was cut with another 7-mm cylindrical knife. The same rings (control samples) were excised from the contralateral cortex of the same rat or from the cortex of a SO animal. These samples were homogenized on ice using a Vibra-Cell VCX 130 ultrasonic homogenizer (Sonics, USA). Nuclear and cytoplasmic fractions were isolated using the CelLyticNuCLEAR Nuclear Fraction Extraction Kit (SigmaAldrich).

Samples containing 10–20 μg of protein per 15 μl were subjected to electrophoretic separation in a polyacrylamide gel (7–10%) in the presence of sodium dodecyl sulfate in a mini-PROTEAN Tetra cell (Bio-Rad, USA). ColorBurst Electrophoresis Marker (C1992, Sigma-Aldrich) was used as standard protein markers. After separation, the proteins were subjected to electrotransfer onto a PVDF membrane (polyvinyl difluoride membrane 162-0177, Bio-Rad) using the Trans-Blot® Turbo Transfer System (Bio-Rad, USA). After washing with PBS, the membrane was successively incubated for 1 hour in blocking buffer (TBS 1% Casein Blocker, Bio-Rad) and overnight at 4°C with primary rabbit antibodies against C-APP (A8717, Merck, 1:500) or N- APP (SAB4200536, Merck, 1:500); anti-ADAM-10, C-terminus (A2726); anti-BACE1 (SAB2100200); anti-nicastrin (ab1) (PRS3983); anti-presenilin-1 (PRS4203); mouse antibodies β-actin (A5441, 1:5000). After incubation, the membranes were washed in Tris buffer with the addition of 0.1% Tween-20 (TTVS, 10 mM; pH 8) and incubated for 1 hour at room temperature with a secondary antibody against rabbit IgG peroxidase (A6154, Merck, 1:1000) . Protein detection was performed on Clarity Western ECL Substrate (Bio-Rad). Chemiluminescence was analyzed using the Fusion SL gel documentation system (Vilber Lourmat, France). The resulting images were processed using the Vision Capt software package.

Cytoplasmic and nuclear fractions of brain tissue extraction

Cytoplasmic and nuclear fractions were obtained using the CelLytic™ NuCLEAR™ Extraction Kit (NXTRACT, Sigma). To do this, the samples were homogenized on ice for 3 minutes using a Vibra-Cell VCX 130 ultrasonic homogenizer (Sonics, USA) in Lysis Buffer, which is included in the CelLytic™ NuCLEAR™ Extraction Kit (NXTRACT, Sigma), supplemented with a mixture of inhibitors proteases and phosphatases (PPC1010, Sigma-Aldrich) necessary for the preservation of proteins and their phosphorylated forms, as well as nuclease benzonase (E1014, Sigma-Aldrich), which destroys nucleic acids. After homogenization, the samples were centrifuged for 20 minutes at 10,000-11,000

 doi:10.20944/preprints202205.0184.v1

x g at 4°C in a Mikro 220R centrifuge (Hettich, Germany). Then, the supernatant containing cytoplasmic proteins was collected, and nuclear proteins were extracted from the sediment containing cell fragments and cell nuclei using the Nuclear Extraction Buffer included in the NXTRACT reagent kit. To do this, the pellet was resuspended and incubated for 40 min with this buffer. After that, the lysate was centrifuged for 5 min at 20,000-21,000 x g at 40C.

In the resulting supernatant containing nuclear proteins and the previously obtained cytoplasmic fraction, the protein content was determined using the Bradford reagent (B6916, SigmaAldrich). The lysates were then aliquoted, frozen in liquid nitrogen and stored at -80°C for further Western blot analysis.

The purity of the fractions was checked as follows: a negative control of the cytoplasmic marker in the nuclear fraction was used, and vice versa, a negative control of the nuclear marker in the cytoplasmic fraction. The acetylated histone protein H4 (ac-H4) was used as a nuclear fraction marker. We used H4 antiacetyl histone obtained from rabbits (No. 06-866, Merck) diluted 1:500. Proteinglyceraldehyde-3-phosphate dehydrogenase (GAPDH) was used as a marker of the cytoplasmic fraction. We used an anti-GAPDH antibody obtained from rabbits (G9545, Sigma-Aldrich) at a 1:1000 dilution. Accordingly, the cytoplasmic fraction was confirmed by the absence of ac-H4, the nuclear fraction was confirmed by the absence of the cytoplasmic fraction marker GAPDH (Figure S1).

Immunofluorescence microscopy

Double immunofluorescence method was used to evaluate the expression and distribution of α-, β- and γ-secretases in penumbra neurons and astrocytes at 24 hours or 7 days after PTS in rats.

The isolated rat brain was fixed in 4% paraformaldehyde overnight and placed in a 30% sucrose solution. Frontal brain sections 20 μm thick (+4.5 mm to -2.5 mm from bregma), obtained using a Leica VT1000 S vibratome (Germany), were washed in PBS and incubated in 5% bovine serum albumin c 0.3% TritonX-100 in PBS for 1 hour at room temperature and then incubated overnight at 4°C in the same BSA solution with antibodies added: anti-ADAM10 (1:500); anti-BACE1 (1:500); anti-nicastrin (ab1) (1:500); anti-presenilin-1 (1:500), as well as antibodies to NeuN (neuron marker) (1:1000), GFAP (astrocyte marker) (1:1000) and caveolin-1 (marker of lipid raft) (1:500). Expression of active caspase 3 and GFAP was assessed by immunofluorescence microscopy as described above. For this, mouse brain sections were incubated with anti-Caspase 3, active (C8487, 1:500) and GFAP (astrocyte marker) (SAB5201104), and then with fluorescent secondary anti-rabbit CF488A (SAB4600045, 1:1000) or anti-mouse antibodies CF555 (SAB4600302) (1:1000). Hoechst 33342 was used as a marker of cell nuclei. After washing in PBS, sections were incubated for 1 hour with fluorescent secondary anti-rabbit CF488A (SAB4600045, 1:1000) or anti-mouse antibodies CF555 (SAB4600302, 1:1000). Sections were then mounted on glass slides in 60% glycerol/PBS. The staining results were analyzed using a Nikon Eclipse FN1 fluorescent microscope (Japan). Quantitative evaluation of the fluorescence of the experimental and control preparations was carried out on 10-15 images obtained with the same digital camera settings. To isolate and calculate the fluorescence intensity, we used the "Threshold" method of the Adjust menu in the Image J program (http://rsb.info.nih.gov/ij/; NIH, USA) as of October 20, 2021. For better isolation, cells were cut off background pixels using the Subtract background feature in the Process menu. Next, using the capabilities of the Analyze Particles and ROI Manager menus, cells were isolated and their total fluorescence intensity was measured. The data was normalized after background subtraction:

$$I = \frac{I_m - I_b}{I_b},$$

 doi:10.20944/preprints202205.0184.v1

I_m - average cell fluorescence intensity, I_b - average background fluorescence outside the cells. Protein colocalization was assessed using the Image J program with the JACoP plugin. The colocalization coefficient M1 reflects the proportion of pixels in the green channels relative to the total signal recorded in the red channel (marker).

Results were analyzed using Nikon Eclipse FN1 fluorescent microscopes (Japan) equipped with a Nikon Digital Sight DS-5Mc digital camera (Japan) with NIS Elements and Olympus BX51 software equipped with an OrcaFlash 4.0 V3 digital camera (Hamamatsu, Japan) with HCImage software live.

Inhibitory assay

Batimastat (batimastat (BB-94); SML0041) was used as an α-secretase inhibitor; β-secretase inhibitor - LY2886721 (SML3013); inhibitor of γ-secretases - DAPT (D5942).

Batimastat was dissolved in DMSO and administered intraperitoneally to CD-1 mice at a dose of 50 mg/kg (or 3 mg/ml) 1 hour after irradiation for 5 days. Batimastat was previously shown to efficiently penetrate the brain when administered intraperitoneally [21].

LY2886721 is a potent and selective active site inhibitor of β-secretase (BACE1,2) without inhibition of other proteases such as cathepsin D, pepsin and renin [22]. The LY2886721 preparation was dissolved in 6.7% DMSO and 5% Tween 20 in PBS and administered to animals intraperitoneally at a dose of 10 mg/kg/day for 5 days.

DAPT, a γ-secretase inhibitor, was dissolved in 5% DMSO and administered to animals intraperitoneally at a dose of 10 mg/kg/day for 5 days [23].

Determination of the volume of cerebral cortex infarction in mice after PTS

To determine the infarct volume at 3, 7, and 14 days after PTS, brain sections of mice were stained with 2,3,5-triphenyltetrazolium chloride (TTX; T8877, Sigma). After decapitation, the brain was quickly removed and placed in a pre-chilled brain matrix of adult mice (J&K Seiko Electronic Co., Ltd). The matrix with brain tissue was transferred to a freezer (-80°C) for 3-5 min and cut into sections 2 mm thick. These sections were stained with 1% TTX for 30 min in the dark at 37°C. Using the Image J image analysis program (http://rsb.info.nih.gov/ij/), the areas of infarction zones on each slice were measured, summed and multiplied by the slice thickness (2 mm).

Estimation of the number of apoptotic cells

Apoptotic cells were visualized using the TUNEL (TdT-mediated dUTP-X nick end labeling) method, which marks DNA strand breaks using the In Situ Cell Death Detection Kit, TMR red (#12156792910, Roche). At 3, 7, and 14 days after PTS and administration of inhibitors, mice were decapitated and frontal sections of the brain 20 μm thick were made on a Leica VT 1000 S vibratome (Germany). The sections were treated with the reagents of the kit in accordance with the manufacturer's recommendations, with the addition of Hoechst 33342 at a final concentration of 10 μg/ml and incubated for 1 hour at 37°C.

The apoptotic index (AI) was calculated for Tunel-positive cells (red fluorescence) in the perifocal region and in the cortex of sham-operated animals along the entire perimeter of the micropreparation at a magnification of 20x using the formula: AI = Number of TUNEL-positive cells/Total number of cells (stained with Hoechst 33342) x one hundred.

Electron immunohistochemistry

Animal brain fixation was performed by transcranial perfusion under anesthesia (Nembutal at a dose of 60 mg/kg) using the Perfusion Two perfusion system (Leica, Germany) equipped with an automatic pump. Perfusion was first carried out with a phosphate buffer solution, pH 7.4, brought to 37°C (Merck, USA), and then with a cooled fixative solution. 4% paraformaldehyde (Merck, EMS, USA) in phosphate buffer (pH 7.4) was used as a fixing solution. The perfusion rate corresponded to the average velocity of

 doi:10.20944/preprints202205.0184.v1

blood movement through the vessels, the total volume of perfusion fluids averaged 200-500 ml. After completion of perfusion, the animal was left alone for 2 hours at room temperature, then the brain or ganglia were removed and placed in a fixative solution (4% paraformaldehyde) for additional fixation overnight at a temperature of 4°C.

After postfixation, a section was isolated from the brain along the coordinates: the first incision was 0.2 mm rostral from the bregma, the second incision was 6.04 mm caudal from the bregma, while the brain was not dissected laterally. The excised brain fragment was glued with the caudal side of the cut down to the vibratome table VT 1000E (Leica, Germany). Next, frontal sections 60 μm thick were made, each of which was placed in a drop of phosphate buffer in a Petri dish and viewed under a stereotaxic magnifying glass in order to detect the stroke area.

Electronic immunohistochemistry was performed on sections of the rat brain, according to the pre-embedding protocol. The pre-embedding method (before embedding) is based on the fact that the incubation of sections with primary and secondary antibodies, as well as the detection of immune complexes, takes place before wiring and embedding the sections in epoxy resin for electron microscopy. 60 μm vibratome sections were placed alternately in solutions of 6%, 15% and 30% sucrose for cryoprotection. Unmasking of antigenic activity was carried out by instantaneous freezing of sections over vapors of liquid nitrogen and subsequent thawing in phosphate buffer. Sections were then incubated in primary anti-APP antibodies supplemented with 0.1% sodium azide to prevent bacterial growth. Incubation was carried out for 4 days at 20°C. After washing in phosphate buffer, the sections were incubated in secondary antibodies RTU Envision Flex/HRP anti-mouse, anti-rabbit (Dako, Denmark) for 24 hours at 20°C. Immune complexes were detected using the EnVision HRP + Peroxidase imaging system (Dako, Denmark). Next, tissue processing was carried out by standard methods for electron microscopic examination. After washing in phosphate buffer (at least 15 minutes), the sections were additionally post-fixed in 1% OsO4 solution in phosphate buffer for 1.5 hours. Further, all tissue samples were dehydrated in ascending alcohols and absolute ethanol, processed in three shifts of propylene oxide, and embedded in an epoxy resin based on Epon-812. The sections were placed in a drop of resin between two glass slides coated with a water-soluble anti-adhesive Liquid Release Agent (EMS, USA). Polymerization of brain tissue was carried out at 70°C overnight. Fragments of the studied zones were excised from the sections obtained after polymerization with a blade under a stereotaxic magnifying glass and polymerized to a prefabricated block of epoxy resin. Single and serial (up to 20 sections in one tape) ultrathin sections 70 nm thick were made using an EM UC 7 ultramicrotome (Leica, Germany) and an ultra 45° diamond knife (Diatome, Switzerland), counterstained with uranyl acetate and lead citrate, and viewed under an electron microscope Jeol 1011 (Jem, Japan) with an accelerating voltage of 80 kV.

Randomization and blinding

Randomization was applied by random choosing of the animals from their cages in vivarium. Blinding was performed when different stages of the experiments (PTS or sham PTS procedure, sacrifice after a certain period post-(sham) PTI, taking brain samples, microscopy, measurement and statistical processing) were performed by different fellow researchers, experimental groups were indicated without specifying their types.

Data collection

The following data were collected:

1) expression levels of C- and N-APP in cytoplasmic fraction of penumbra tissue in 4 and 24 hours post-PTS in ipsilateral (PTS) and contralateral area and in sham-operated control;

2) electron immunohistochemistry microscopy images in 4 and 24 hours post-PTS and in controls for visual analysis of intracellular localization of C- and N-APP;

 doi:10.20944/preprints202205.0184.v1

3) expression level of ADAM10 protein in cytoplasmic fraction and its colocalization rate with NeUN, GFAP, and caveolin in penumbra 4h, 24h, 7 days post-PTS, and in control;

4) expression levels of BACE1, PS1, and nicastrin proteins in cytoplasmic fraction and their colocalization rate with NeUN, GFAP, in penumbra 4h, 24h, 7 days post-PTS, and in control;

5) infarction volume, apoptotic index, and levels of active caspase-3 and GFAP in 7 and 14 days post-PTS in animals pretreated with secretase inhibitors BB-94, LY2886721, DAPT, and without pretreatment (PTS-only control).

Table 1. Time duration from photothrombotic stroke induction to the different methods of data collection

Time post-PTS	4h	24h	3d	7d	14d
Immunoblotting (rats)	✓	✓		✓	
Immunofluorescence microscopy (rats)	✓	✓		✓	
Electronic immunohistochemistry (rats)	✓	✓			
Immunofluorescence microscopy (mice)			✓	✓	✓
Infarction area estimation (mice)			✓	✓	✓
TUNEL (mice)			✓	✓	✓

Statistical analysis

In studies with a single effective factor (time post-PTS), differences between sample groups were statistically estimated using one-way ANOVA (Fig. 2-9). In studies where different-target inhibitors were used (secretase types in Fig. 10) we applied Student's t-test.

For a posteriori (post hoc) test in ANOVA, Tukey Holm-Sidak's test was applied with all-pairwise (for three 4h groups and for three 24h independently in Fig. 2) or with versus control comparison type (Fig 3-9). Differences were considered significant at $p<0.05$. Data were presented as Mean ± SEM.

3. Results

APP expression in the rat cerebral cortex after PTS

According to immunoblotting data, PTS stimulates the accumulation of the C-terminal APP fragment in the ischemic penumbra. In the cortex of control animals, the level of C-APP in the cytoplasmic fraction is not high (Fig. 2a). At 4 hours after PTS, the

Preprints (www.preprints.org) | NOT PEER-REVIEWED | Posted: 13 May 2022 doi:10.20944/preprints202205.0184.v1

level of C-APP in the penumbra tissue did not differ from the control. However, after 24 hours it significantly increased in the cytoplasmic fraction (Fig. 2a).

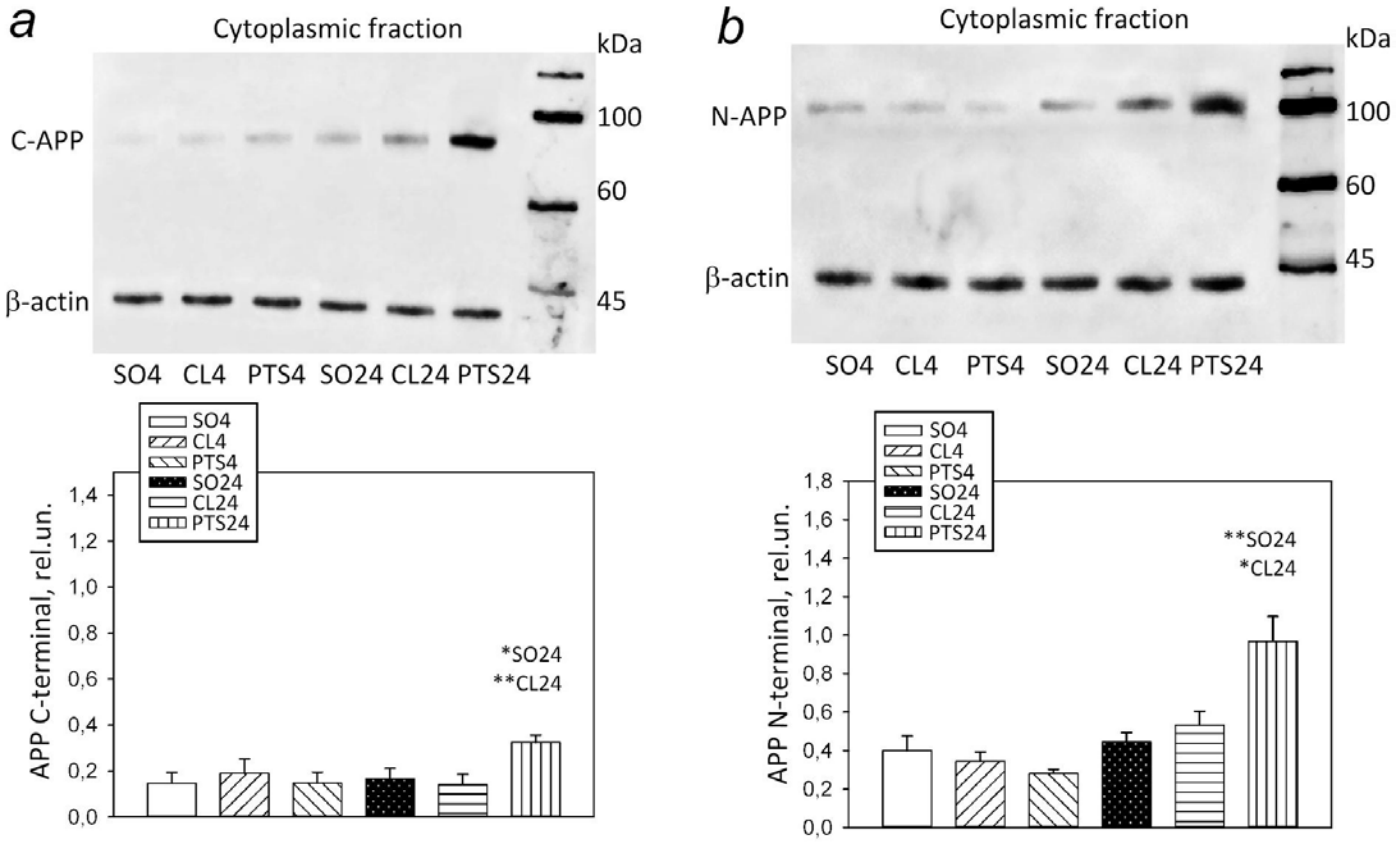

Figure 2. *a*) The level of C-APP in the cytoplasmic fraction of penumbra tissue at 4 and 24 hours after photothrombotic stroke in the cerebral cortex of rats. *b*) N-APP levels in the cytoplasmic fraction of penumbra tissue at 4 and 24 hours after photothrombotic stroke in the rat cerebral cortex. Control groups: the contralateral cortex of the same rats (CL4 and CL24, respectively) and the cerebral cortex of sham-operated rats (SO4 and SO24). OneWay ANOVA. M ± SEM. $n = 7$. * $p < 0,05$; ** $p < 0,01$.

The level of N-APP was also low in the cytoplasmic fraction. However, at 24 hours but not at 4 hours after PTS it significantly increased (Fig. 2b).

The accumulation of N-APP in the cytoplasm at 24 hours after PTS indicates an increased synthesis of the APP protein in neurons, or its slow export to the plasma membrane that could be due to impaired vesicular transport.

A more detailed picture of the intracellular distribution of the APP protein is provided by electron immunohistochemistry data.

Subcellular distribution of N- and C-terminal fragments of APP in rat brain cells in normal conditions and on the first day after photothrombotic stroke

In brain samples of sham-operated rats after an immunohistochemical reaction with antibodies to APP fragments, it was shown that reaction products in thin unmyelinated processes are visualized in the cerebral cortex. The N- and C-terminal fragments of APP are also found in large processes containing mitochondria. In addition to cut axons and dendrites along and across, there are active zones of chemical synapses in the field of view, while it seems that the reaction products accumulate in the postsynaptic part (Fig. 3a).

 doi:10.20944/preprints202205.0184.v1

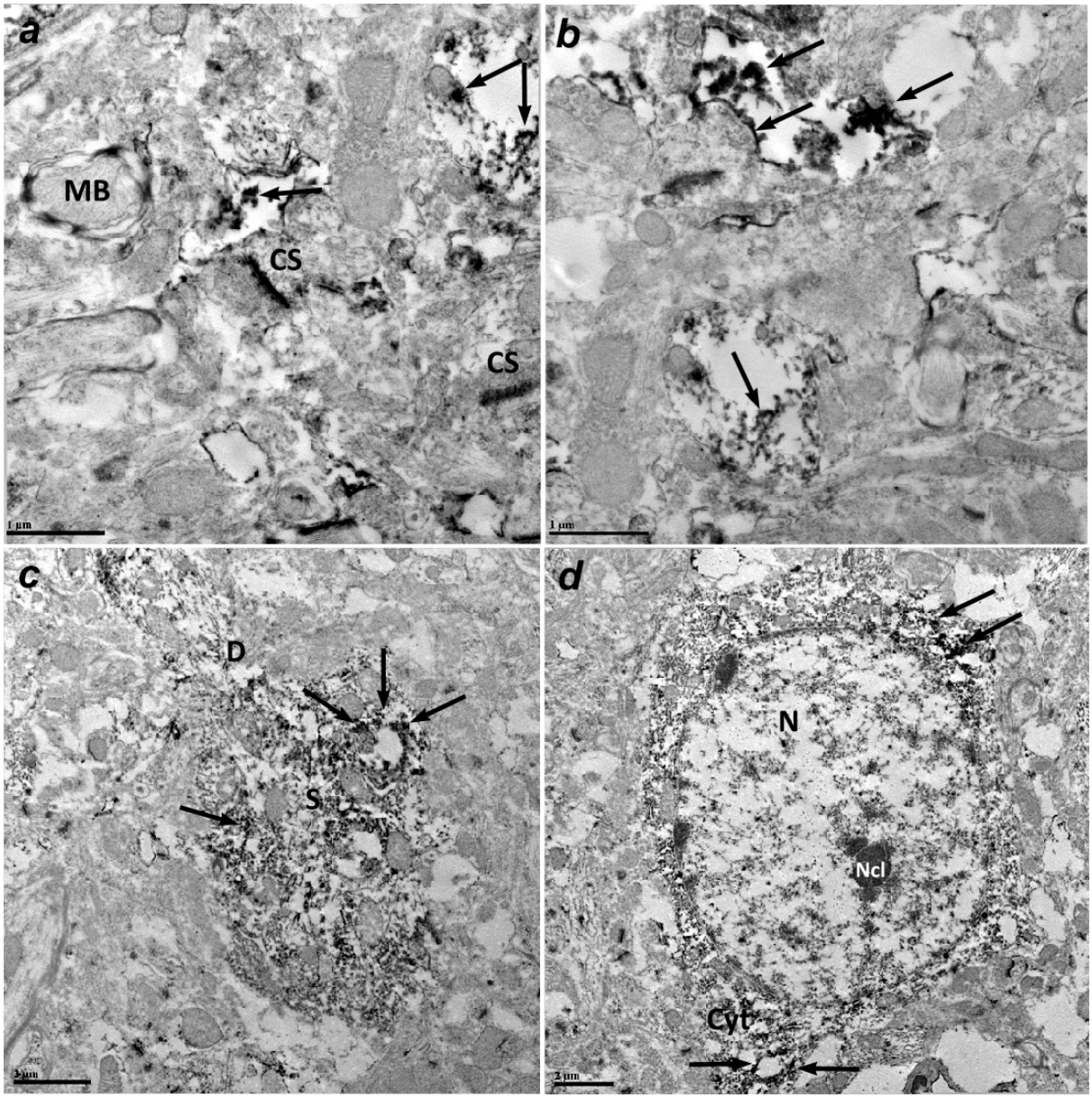

Figure 3. Electron immunohistochemistry with antibodies to C- and N-terminal fragments of APP protein in rat brain neocortex of control group (a,b) and 4 hours after photothrombotic stroke (c,d). a – Localization of APP (C-terminal domain): medium amount of protein associated with cellular elements. b - Localization of APP (N-terminal domain): filling of individual cell processes with APP protein. c - APP (N-terminal domain) localization: numerous processes containing APP fragments. d - APP (N-terminal domain) localization in neuronal cytoplasm. Legent: CS – chemical synapse, MB – mielin branch, S- neuronal soma, D – dendrite, N- nucleus, Ncl- nucleolus, Cyt- cytoplasm, the products of reaction are indicated by arrows. Magnification: a,b x50 000 (Scale bar 1 mkm); c,d x20 000 (Scale bar 2 mkm).

In some cases, processes are observed that absorb a larger amount of electron-dense flocculent material - the result of immunohistochemical reactions. The reaction products are also coupled to the plasma membranes of the processes (Fig. 3c).

Electron microscopic examination of the brain neuropil after a 4-hour photothrombotic stroke and the study of the expression of the N- and C-ends of APP showed that both of them accumulate both in the processes and in the cytoplasm of individual neurons (Fig. 3c).

At lower magnifications, the ubiquitous localization of APP protein fragments in the neuropil was observed - in the longitudinally and transversely cut dendrites of neurons,

Preprints (www.preprints.org) | NOT PEER-REVIEWED | Posted: 13 May 2022 doi:10.20944/preprints202205.0184.v1

as well as in processes with the absence of organelles and single mitochondria (presumably glial processes), the zone of chemical synapses (Fig. 3d).

Individual neurons containing APP fragments come across in the field of view. Such neurons contain nuclei without APP with several nucleoli, as well as the cytoplasm, with evenly distributed N- and C-terminal fragments of the APP protein in it (Fig. 3c, 3d).

After a 24-hour photothrombotic stroke, significant tissue damage occurred: lysis of nuclei, destruction of cells and processes. At the same time, some elements of the destroyed tissue accumulated a significant amount of the APP protein (Fig. 4).

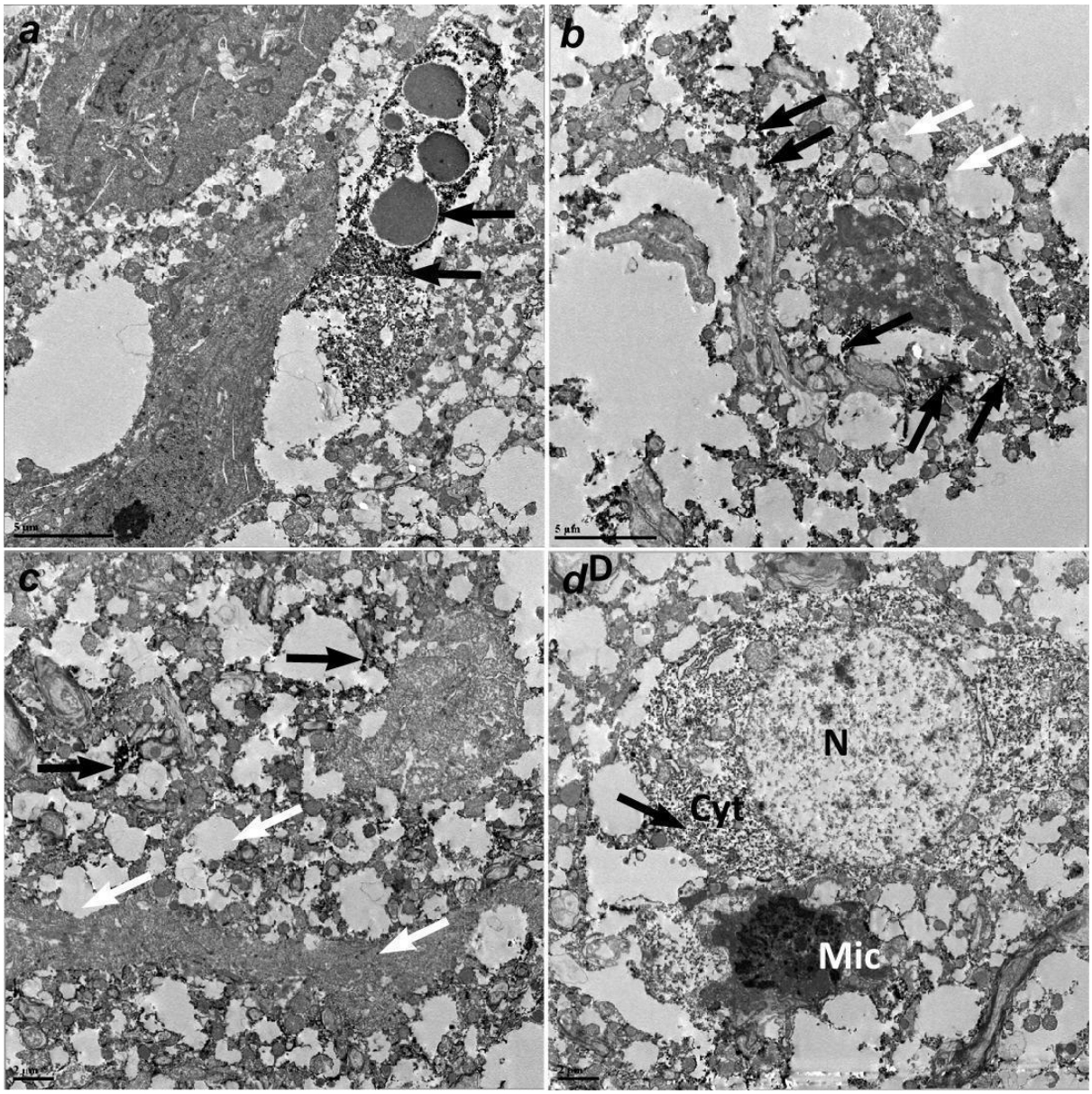

Figure 4. Electron immunohistochemistry with antibodies to C- and N-terminal fragments of APP protein in rat brain neocortex at 24 hours after photothrombotic stroke (a,c - C domain, b,d - N domain). a - destruction of the neuropil. b - lysis of the cytoplasm of the cell and processes. c- the destroyed processes in the neuropil contain an intense amount of the APP protein. d - A neuron containing the APP protein and an APP-negative microglial cell. Legent: N- nucleus, Cyt- cytoplasm, Mic – microglia, the products of reaction are indicated by arrows. Magnification: a and b x10 000 (Scale bar 5 mkm); c,d x20 000 (Scale bar 2 mkm).

Even in the destroyed tissue the reaction products were localized mainly in the cytoplasm; neuropil elements negative for the APP protein were also visualized (Fig. 4b).

Preprints (www.preprints.org) | NOT PEER-REVIEWED | Posted: 13 May 2022 doi:10.20944/preprints202205.0184.v1

For example, a neuron containing the APP protein in the cytoplasm and a microglial cell with a dark nucleus negative for the APP protein is localized among the destroyed tissue (Fig. 4d).

Thus, the reaction products of both the C-terminal and N-terminal fragments of APP accumulate in thin processes, axons and dendrites, as well as in the zones of chemical synapses. At the ultrastructural level, there were no differences in the localization or accumulation dynamics of the C- or N-terminal APP fragment. At the level of individual neurons, APP protein fragments are associated with the cell cytoskeleton, rough endoplasmic reticulum, ribosomes, and are absent in nuclei. The intensity of the reaction products depends on the time after exposure. Nerve cells contained the greatest amount of protein at 24 hours after PTS. However, some glial cells and neurons did not accumulate the APP protein. Further, it is necessary to understand which cells do not contain APP and why.

Expression of ADAM10 in the rat cerebral cortex after photothrombotic stroke

According to immunoblotting data, α-secretase ADAM10 is mainly present in the cytoplasmic fraction of the penumbra tissue (Fig. 5). In the nuclear fraction, the protein is contained in trace concentrations. A sufficiently high level of protein is noted in the sham-operated animals and at 4 hours after PTS. At 24 hours after PTS the level of ADAM10 decreased by a factor of 2 times ($p<0.01$) in the cytoplasmic fraction relative to sham-operated animals. On day 7, PTS caused a significant increase in ADAM10 in the cytoplasmic fraction by 97% ($p<0.01$) relative to the protein level at one day after PTS, approaching the values of the group of sham-operated animals (Fig. 5).

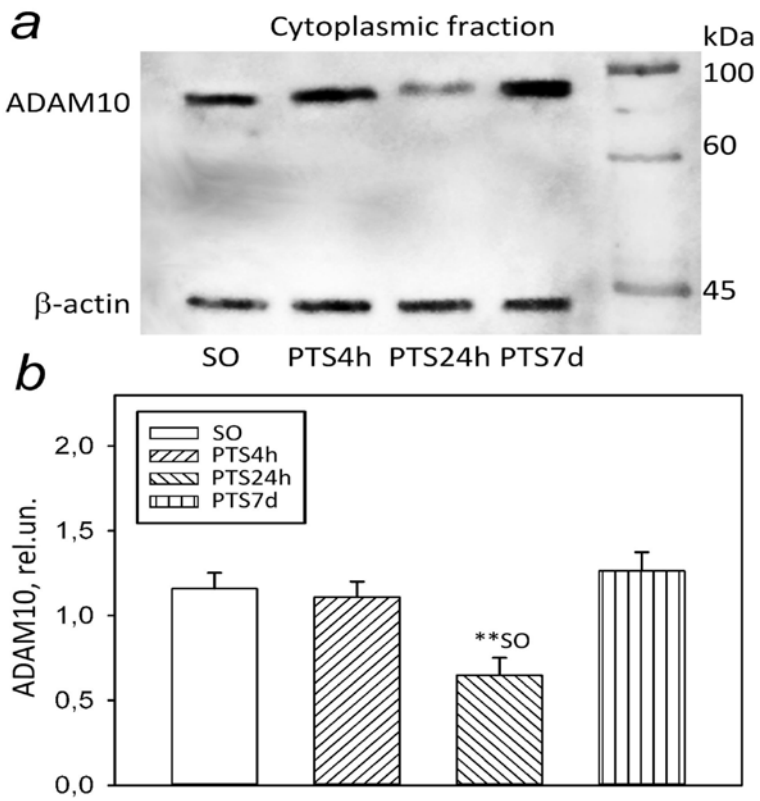

Figure 5. a) ADAM10 in the cytoplasmic fraction of the cortex of sham-operated animals (SO) and at 4 (PTS 4h), 24 (PTS 24 h) and 7 days (PTS 7d) after PTS; b) ADAM10 level in conventional units at different times after PTS. The indices of the groups of sham-operated animals at 4, 24 hours and 7 days after irradiation had no statistically significant differences, therefore the indices of the three groups were combined. OneWay ANOVA. M ± SEM. n = 6-8. ** p <0,01.

Preprints (www.preprints.org) | NOT PEER-REVIEWED | Posted: 13 May 2022 doi:10.20944/preprints202205.0184.v1

A more detailed picture of the intracellular distribution of the protein is provided by immunofluorescence microscopy data. The immunofluorescence signal of ADAM10 in brain tissue is low. ADAM10 expression in neurons, but not in penumbra astrocytes of sham-operated animals, is quite high (Fig. 6 a, c, d). The protein is localized mainly in the cytoplasm of neurons.

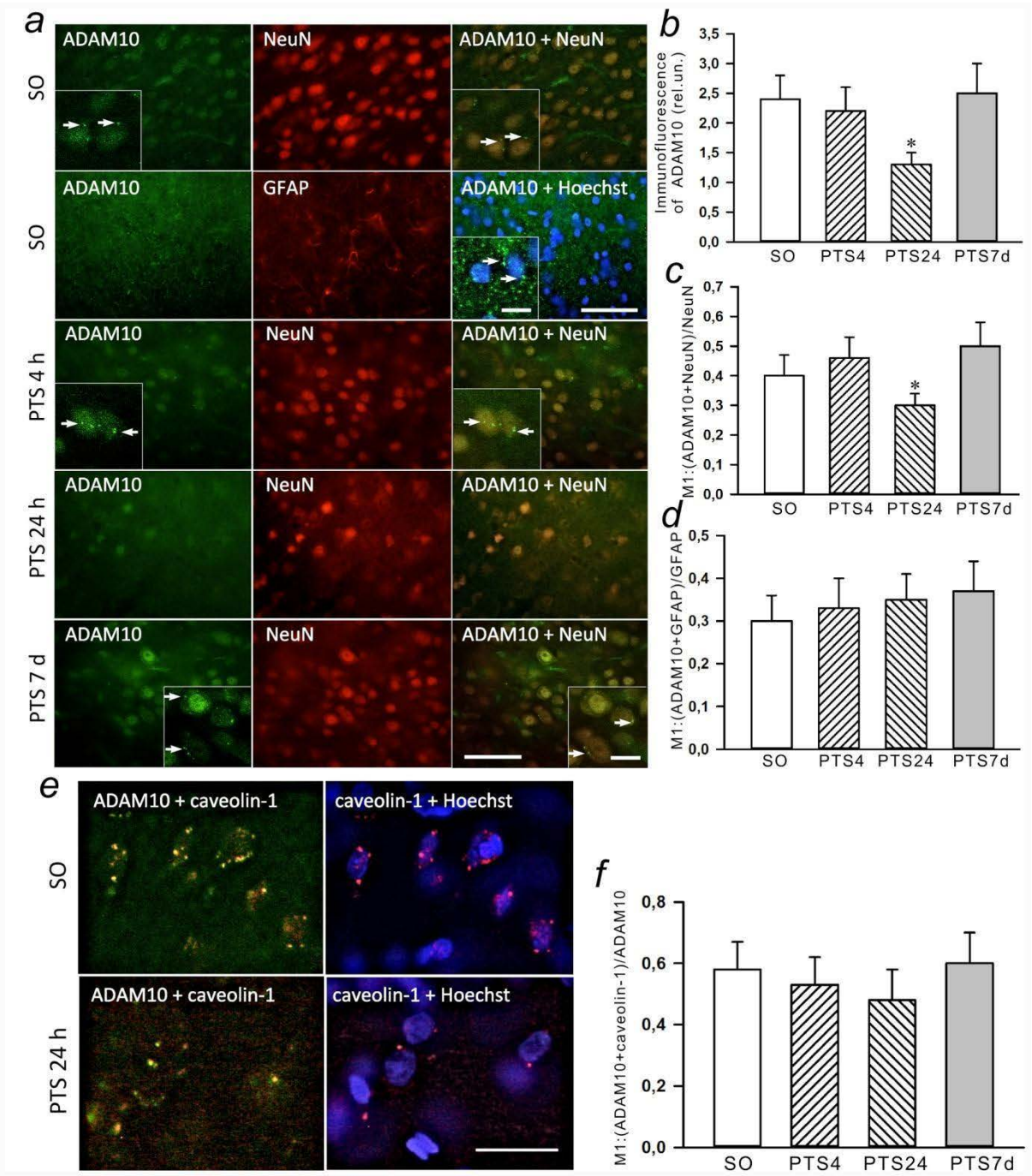

Figure 6. Changes in ADAM10 expression in the penumbra at 4, 24 hours and 7 days after PTS in the rat cerebral cortex (PTS4h, PTS24h and PTS 7d, respectively) relative to the cortex of sham-operated rats (SO). a) ADAM10 (green) and NeuN (red) or GFAP (red) immunofluorescence and image overlay. Scale bar 100 μm. Insert: enlarged image. Scale bar 50 μm. Arrows show granularity (clusters) in the area of the cytoplasmic membrane. b) ADAM10 fluorescence in penumbra cells after PTS and in the cortex of sham-operated rats.* p <0,05 compared to the SO. c) Localization of ADAM10 in penumbra neurons. d) Localization of ADAM10 in penumbra astrocytes. e) Image overlay ADAM10 (green) and caveolin-1 (red) or caveolin-1 (red) and Hoechst (blue)

Preprints (www.preprints.org) | NOT PEER-REVIEWED | Posted: 13 May 2022 doi:10.20944/preprints202205.0184.v1

immunofluorescence and image overlay. Scale bar 50 μm. f) Co-localization of ADAM10 and caveolin-1 (Manders coefficient M1). OneWay ANOVA. M ± SEM. *n* = 6-8. * p <0,05 compared to the SO.

At 24 hours after PTS an almost 2-fold decrease in the level of ADAM10 compared with the control level is observed due to its decrease in neurons (Fig. 6c), but not in penumbra astrocytes (Fig. 6d).

Noteworthy is the clustering of ADAM10 on the surface of the cytoplasmic membrane. ADAM10 is known to be able to translocate into caveolin-1-enriched lipid rafts, which serve as a platform for signaling proteins and initiate intracellular signaling events [24]. Therefore, we conducted studies of ADAM10 colocalization with caveolin-1 that allowed us to more accurately describe the nature of ADAM10-containing clusters on the surface of cerebral cortex cell membranes. Immunofluorescence microscopy study showed that co-localization of caveolin-1 with ADAM10 was indeed observed (Fig. 6e), and the coefficient of co-localization of M1 proteins did not change at different timepoints after PTS (Fig. 6f).

Expression of BACE1 in the rat cerebral cortex after photothrombotic stroke

β-secretase BACE1 is practically absent in the nuclear fraction of rat cerebral cortex cells. Our study of BACE1 expression by Western blot at different times after PTS did not reveal any change in the content of BACE1 in the cytoplasmic fractions of the penumbra tissue compared to the group of sham-operated animals (Fig. 7 a,b).

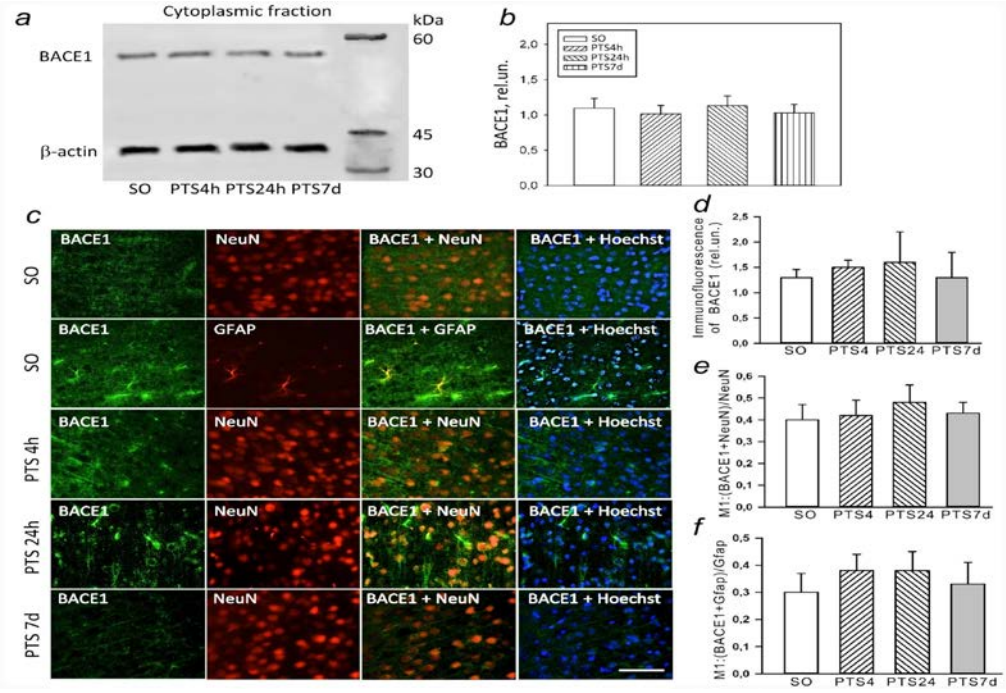

Figure 7. a) Immunoblotting of BACE1 in the cytoplasmic fractions of the cortex of sham-operated animals (SO) and at 4 (PTS 4h), 24 (PTS 24 h) and 7 days (PTS 7d) after PTS; b) BACE1 level in relative units at different times after PTS. The indices of the groups of sham-operated animals at 4, 24 hours and 7 days after PTS had no statistically significant differences, therefore the indices of the three groups were combined; c) Changes in BACE1 expression in the penumbra at 4, 24 hours and 7 days after PTS in the rat cerebral cortex (PTS4h, PTS24h and PTS 7d, respectively) relative to the cortex of sham-operated animals (SO). BACE1 (green) and NeuN (neuron marker, red) or GFAP (astrocytes marker, red) or Hoechst (nuclei marker, blue) immunofluorescence and image overlay. Scale bar 100 μm. d) Changes (in relative units) in BACE1 fluorescence in penumbra cells after PTS and in the cortex of sham-operated rats. e) Localization of BACE1 in penumbra neurons. f) Localization of BACE1 in penumbra astrocytes. OneWay ANOVA. M ± SEM. *n* = 8.

Preprints (www.preprints.org) | NOT PEER-REVIEWED | Posted: 13 May 2022 doi:10.20944/preprints202205.0184.v1

The results of immunofluorescent analysis also did not reveal changes in BACE1 expression in both neurons (Fig. 7e) and astrocytes (Fig. 7f) of the penumbra on the first day and in the early recovery period after a PTS (Fig. 7 c,d).

BACE1 expression in neurons and astrocytes of the rat cerebral cortex was not high, as indicated by Western blot data.

Presenilin-1 expression in the rat cerebral cortex after photothrombotic stroke

According to Western blot analysis, the level of presenilin-1 in both fractions of the cortex of sham-operated animals was low. However, there is an increase in the protein level in the cytoplasmic fraction of the penumbra tissue at 4 hours after photothrombotic exposure (by 49%, $p<0.5$) (Fig. 8 a,b). After 24 hours, protein overexpression in the cytoplasmic fraction increased by a factor of 2.5 compared to control ($p<0.01$) and by factor of 1.5 relative to the protein level at 4 hours after PTS ($p<0.01$) (Fig. 8 a,b). On day 7 after PTS the protein level in the cytoplasm of penumbra cells significantly decreased compared to 24 hours after PTS, returning to control values (Fig. 8 a,b).

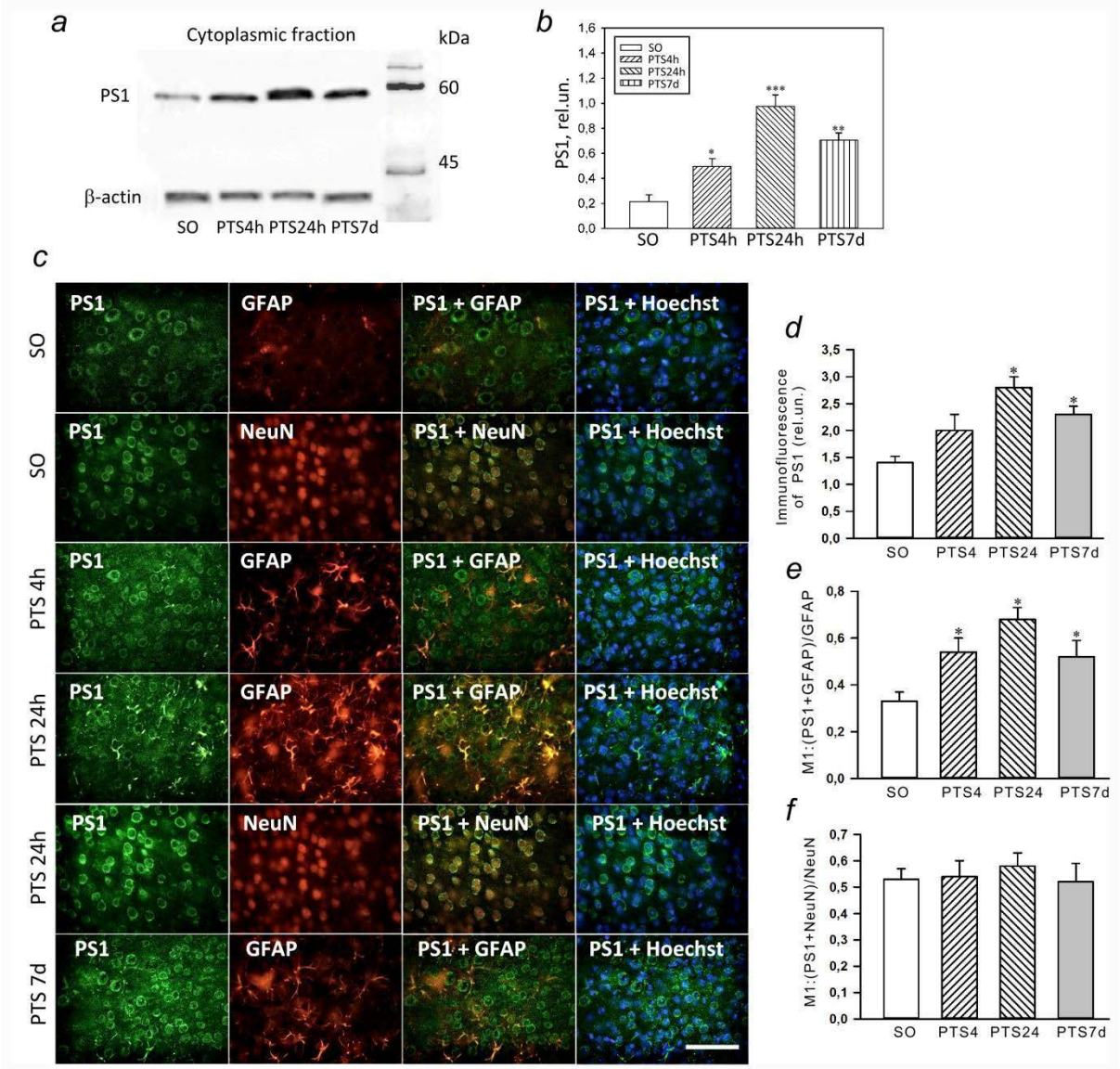

Figure 8. a) Immunoblotting of presenilin-1 (PS1) in the cytoplasmic fraction of the cortex of sham-operated animals (SO) and at 4 hours (PTS 4h), 24 hours (PTS 24 h) and 7 days (PTS 7d) after PTS; b) PS1 level in relative units at different timepoints after PTS. The indices of the groups of sham-operated animals at 4, 24 hours and 7 days after PTS had no significant differences, therefore the

 doi:10.20944/preprints202205.0184.v1

indices of the three groups were combined. c) Changes in PS1 expression in the penumbra at 4, 24 hours and 7 days after PTS in the rat cerebral cortex (PTS4h, PTS24h and PTS 7d, respectively) relative to the cortex of sham-operated animals (SO). PS1 (green) and GFAP (astrocytes marker, red) or NeuN (neuron marker, red) or Hoechst (nuclei marker, blue) immunofluorescence and image overlay. Scale bar 100 μm. d) Changes (in relative units) in PS1 fluorescence in penumbra cells after PTS and in the cortex of sham-operated rats. e) Localization of PS1 in penumbra astrocytes. f) Localization of PS1 in penumbra neurons. OneWay ANOVA. M ± SEM. *n* = 6-8. *p≤0,5; **p≤0,01; ***p≤0,001 compared to the SO.

Immunofluorescent analysis shows that the increase in presenilin-1 expression is associated with its growth in astrocytes, but not in penumbra neurons (Fig. 8 c,e,f). The dynamics of changes in the colocalization coefficient of presenilin-1 with the astrocyte marker GFAP was almost the same as in the total cytoplasmic fraction according to Western blot analysis (Fig. 8b).

In neurons, presenilin-1 is localized exclusively in the cytoplasm, both in normal conditions and after PTS (Fig. 8c). An increase in the protein level on the first day after PTS, which persisted during the recovery period, was not associated with its growth in neurons, since the colocalization of presenilin-1 with the neuronal marker NeuN did not differ significantly from that in sham-operated animals (Fig. 8f).

Expression of nicastrin in the rat cerebral cortex after photothrombotic stroke

Like presenilin-1, nicastrin is part of the γ-secretase protein complex. Little is known about the function of nicastrin in neuronal injury after stroke. In the course of proteomic studies, we have shown an increase in the expression of nicastrin in the penumbra on the first day after a photothrombotic stroke [4].

According to immunoblotting data, the initial level of the nicastrin protein in the cytoplasmic fraction of the cortex of sham-operated animals was not high (Fig. 9a). In the nuclear fraction, the protein was practically not identified. At 4 hours after PTS the protein level increased by a factor of 6 relative to sham-operated animals in the cytoplasmic fractions of the penumbra tissue (Fig. 9b). At 24 hours after PTS the protein level in the cytoplasmic fraction still continued to rise and was higher by a factor of 10 compared to the control value ($p<0.01$) and by a factor 6 times compared to the protein level at 4 hours after PTS($p<0.01$) (Fig. 9a). The level of nicastrin at 7 days after PTS significantly decreased compared to 4 and 24 hours after PTS but still remained higher than the control group ($p<0.05$) (Fig. 9b).

Preprints (www.preprints.org) | NOT PEER-REVIEWED | Posted: 13 May 2022 doi:10.20944/preprints202205.0184.v1

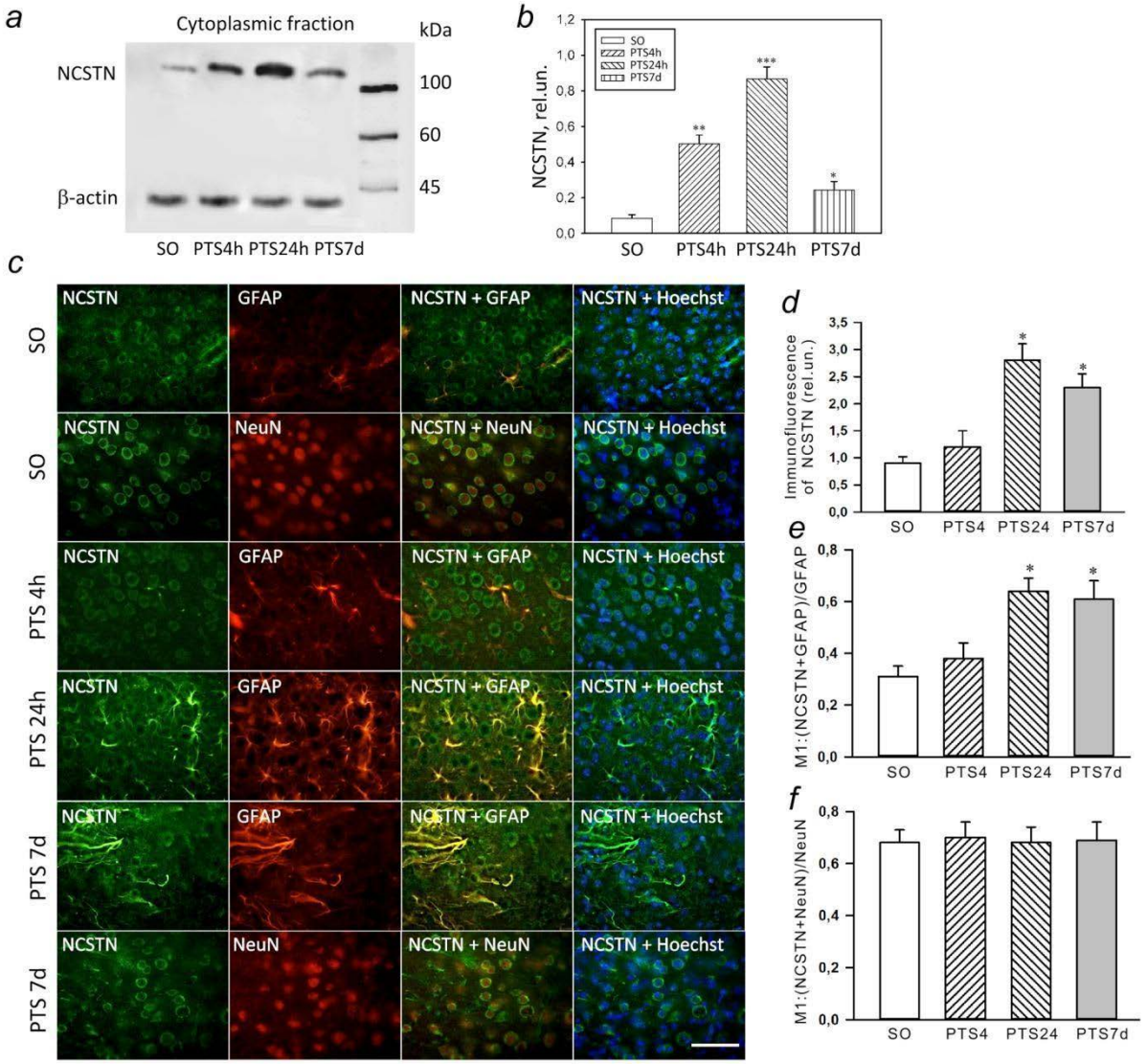

Figure 9. a) Immunoblotting of nicastrin (NCSTN) in the cytoplasmic fraction of the cortex of sham-operated animals (SO) and at 4 (PTS 4h), 24 (PTS 24 h) and 7 days (PTS 7d) after PTS; b) Nicastrin level in conventional units at different timepoints after PTS. The indices of the groups of sham-operated animals at 4, 24 hours and 7 days after PTS had no statistically significant differences, therefore the indices of the three groups were combined. c) Immunofluorescence of nicastrin (NCSTN) (green) and GFAP (astrocyte marker, red) or Hoechst (nuclei marker, blue) and image overlay in sham-operated animals (SO) and at 4 (PTS 4h), 24 (PTS 24 h) and 7 days (PTS 7d) after PTS. Scale bar 100 μm. d) Changes (in conventional units) of nicastrin fluorescence in penumbra cells after PTS and in the cortex of sham-operated rats. e) Localization of nicastrin in penumbra astrocytes. f) Localization of NCSTN in penumbra neurons. OneWay ANOVA. M ± SEM. n = 6-8. *p≤0,5 compared to the SO..

The data of fluorescent microscopic studies confirm the conclusions of the Western blot analysis. Nicastrin is present in the cytoplasm of neurons and nuclei, cytoplasm and processes of astrocytes. Although there is a lot of protein in the brain cells of sham-operated animals, its level increases after PTS (Fig. 9c). An increase in the level of nicastrin is observed at 24 hours and persists up to 7 days after PTS (Fig. 9d). At the same time, an increase in protein expression is associated with its high content in astrocytes (Fig. 9e), but not in penumbra neurons (Fig. 9f).

Thus, the expression of the main proteins of the γ-secretase complex: presenilin-1 and nicastrin increases in penumbra astrocytes on the first day after a stroke and in the

Preprints (www.preprints.org) | NOT PEER-REVIEWED | Posted: 13 May 2022 doi:10.20944/preprints202205.0184.v1

early recovery period, which is probably due to their participation in the reaction of astrocytes to damage and during repair after a stroke.

Effect of α-, β-, and γ-secretase inhibitors on infarct volume and apoptosis level in the brain of mice after photothrombotic stroke

Batimastat or BB-94 was used as an α-secretase inhibitor. The inhibitor molecule mimics the metalloproteinase substrate and therefore acts by competitive reversible inhibition [28]. In a number of studies, BB-94 is used to study APP processing [29] and the role of its proteolytic products in memory processes and the pathogenesis of AD [30]. In addition, metalloproteinases are currently considered as effective antitumor agents [28], which was confirmed by experiments with the administration of batimastat in rodent tumor models [28, 31]. Batimastat is almost completely insoluble and therefore has very low oral bioavailability. Thus, the only way to administer batimastat is by direct injection into various body cavities (abdominal and pleural) [28]. In our work on PTS model in mice batimastat (SML0041, Sigma-Aldrich) was dissolved in DMSO and administered to animals intraperitoneally at a dose of 50 mg/kg (or 3 mg/ml) one hour after irradiation once a day for 5 days [28, 32-34]. It has been previously demonstrated that BB-94 efficiently enters the brain when administered intraperitoneally [34, 35]. The selected dose of BB-94 has been shown to work in a mouse model of focal cerebral ischemia [23, 34]. Also, similar doses are effective in rodent tumor models [31]. However, we failed to detect the effect of the drug on changes in infarct volume, caspase-3 expression, or the level of apoptosis of mouse cerebral cortex cells (Fig.10).

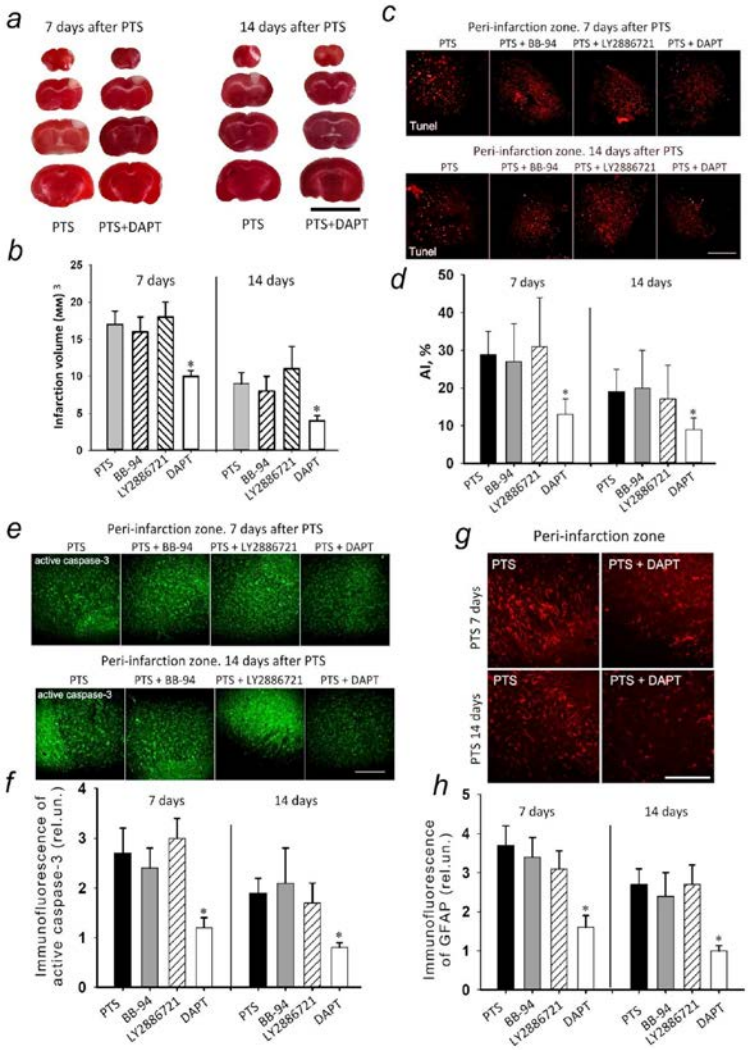

 doi:10.20944/preprints202205.0184.v1

Figure 10. Effects of secretase inhibitors: LY2886721 - inhibitor of β-secretases BACE1 and BACE2; DAPT is an inhibitor of γ-secretase on the volume of the infarct nucleus, apoptosis and expression of GFAP in the peri-infarction region of PTS in the mouse cerebral cortex on days 7 and 14 after PTS. a) View of sections of the mouse brain 7 and 14 days after PTS and against the background of the introduction of DAPT stained with TTS. The dotted line is the zone of infarction. b) Average values of the infarct core volume (mm^3) in the control groups (PTS without inhibitors) and in the experimental groups (administration of inhibitors) 7 and 14 days after PTS. Scale bar 1 cm. c) Representative images of cortical areas stained with TUNEL (red fluorescence of apoptotic cells) 7 and 14 days after PTS. Experimental groups: BB-94, inhibitor of α-secretase ADAM10; LY2886721, inhibitor of BACE1 and BACE2 β-secretases; DAPT is a γ-secretase inhibitor. Scale bar 200 μm. d) Changes in the apoptotic index (AI, %) in mice 7 and 14 days after PTS and after administration of inhibitors. e) Immunofluorescence of active caspase-3 (green) in the peri-infarction region of PTS in the mouse cerebral cortex on days 7 and 14 after PTS and against the background of the introduction of DAPT. Scale bar 200 μm. f) Changes (in conventional units) of active caspase-3 fluorescence in the peri-infarction region of PTS and against the background of the introduction of inhibitors. g) Immunofluorescence of GFAP (red) in the peri-infarction region of PTS in the mouse cerebral cortex on days 7 and 14 after PTS and against the background of the introduction of DAPT. Scale bar 200 μm. h) Changes (in conventional units) of GFAP fluorescence in the peri-infarction region of PTS and against the background of the introduction of inhibitors. T-test. M ± SEM. n = 7-10. *p≤0,5 compared to the PTS..

LY2886721 is a potent and selective active site inhibitor of β-secretase (BACE1,2) without inhibition of other proteases such as cathepsin D, pepsin and renin [36,37].

Here in a model of PTS in mice, LY2886721 was dissolved in 6.7% DMSO and 5% Tween 20 in PBS and administered to animals intraperitoneally at a dose of 10 mg/kg/day for 5 days. As in the case of batimastat, we failed to detect the effect of LY2886721 on changes in infarct volume or the level of apoptosis of mouse cerebral cortex cells after photothrombotic stroke (Fig. 10 a,b,c,d).

DAPT (N-[N- (3,5-difluorophenacetyl)-1-alanyl]-Sphenylglycine t-butylester) is a γ-secretase inhibitor. The dose of DAPT was selected based on literature data [38] and verified in preliminary experiments. The drug was dissolved in 5% DMSO and administered to animals intraperitoneally at a dose of 10 mg/kg/day for 5 days. Of the three secretase inhibitors studied, only DAPT reduced the infarct volume on days 7 and 14 after PTS, preventing the growth of mouse cerebral cortex cell apoptosis in the area adjacent to the infarction zone (Fig. 10).

In this work, we have shown that photothrombotic stroke causes an increase in the level of γ-secretase protein subunits of presenilin-1 and nicastrin in astrocytes, but not in penumbra neurons. In this regard, we evaluated the expression of GFAP in astrocytes of the perifocal region adjacent to the infarction zone after PTS and after the administration of the γ-secretase inhibitor, DAPT. The inhibitor was shown to reduce the level of GFAP in cortical astrocytes (Fig. 10 g,h). At the same time, the effect was already pronounced on the 3rd day after the administration of the drug and persisted up to 7 days after the PTS (Fig. 10h).

4. Discussion

An electron microscopic study showed that in the cells of the cortex of sham-operated rats, N- and C-terminal fragments of APP are visualized both in thin unmyelinated fibers of neurons and in large fibers containing mitochondria in the postsynaptic part of chemical synapses. As early as 4 hours after PTS, a clear difference was shown in the accumulation of the APP protein (C- and N-terminal domains of the protein) among various cellular elements. Thus, glial elements (shells, nuclei, cytoplasm) were negative for APP, and elements belonging to neurons intensively accumulated this protein. 24 hours after PTS, some elements of the destroyed tissue accumulate a significant amount of APP protein, but there are cells that do not contain APP fragments, such as microglial cells (Fig. 4d). The reasons for this selective expression of APP in different cell types remain to be elucidated. It is known that mice lacking APP and BACE1 have a higher risk

 doi:10.20944/preprints202205.0184.v1

of death after cerebral ischemia. In APP knockout mice, cerebral blood flow is reduced after hypoxia due to a decrease in serum response factor (SRF) and the calcium-binding protein calsequestrin, which are involved in vascular regulation. All this indicates the important role of APP and its fragments in the regulation of blood flow in the brain and are crucial for rapid adaptation [35].

The non-amyloidogenic proteolysis of APP, which results in the formation of the large amino-terminal domain of APP and CTFα (C83), is carried out by a set of proteases called α-secretases. α-secretases are associated with the plasma membrane [11]. The proteinases of the "disintegrin and metalloproteinases" or ADAM family, such as ADAM9, ADAM10, TACE/ADAM17, and ADAM19, act as α-secretase in mammalian cells [14]. However, in neurons, α-secretase activity is associated with ADAM10 [36]. In addition to APP, α-secretases cleave Notch receptors and ligands, tumor necrosis factor α, cadherins, the IL-6 receptor, EGF receptor ligands, and several other transmembrane proteins to release their extracellular domain [37]. Protein kinase C is known to stimulate the processing of α-secretases and the secretion of the APP ectodomain [11]. Thus, the activity of α-secretases is closely associated with intracellular signaling in brain cells both in normal and pathological conditions, as evidenced by the observed colocalization of ADAM10 with the lipid raft marker caveolin-1. Previously, it was shown that ADAM10 expression significantly increased at the early stage of cultivation of human neuroblastoma cell line neurons and primary cultured cells of transgenic mice expressing human APP (Tg2576) under conditions of oxygen and glucose deprivation, but then followed by a decrease in the level of ADAM10 expression in the recovery stage [39]. Chronic cerebral hypoperfusion caused an increase in the levels of sAPPα, ADAM10, and ADAM17 in the hippocampus of rats against the background of an even more significant increase in the levels of sAPPβ, BACE, and BACE1, which contributed to the stimulation of the amyloidogenic pathway of APP processing and caused cognitive impairment [25]. However, in a model of ischemic stroke in rats caused by PTS a decrease in the enzyme in neurons occurred on the first day after a stroke, but by the 7th day the protein level is restored to control values. Perhaps this is due to a general decrease in protein biosynthesis, which is not needed during the most acute period of stroke. Unlike ADAM17, ADAM10 is not known to be involved in myelination during development or in remyelination after injury. ADAM10 is required in neurons during axon regeneration in vivo [40]. In addition, the SIRT1/ERK/NF-κB signaling pathway has recently been shown to contribute to the suppression of ADAM10, leading to a switch from non-amyloidogenic to amyloidogenic APP processing under conditions of oxidative stress [41].

It is known that ADAM10 overexpression in neurons in transgenic mice reduces the processing of BACE1 β-secretase and amyloid deposition [11]. However, using two different methods, we were not able to show the increase of BACE1 level in the brain after PTS, both during the acute period and during the recovery period, which is indicated by the literature data [25-27]. Perhaps this is due to the peculiarity of the photothrombosis model, in which there is no complete reperfusion [18]. It is known that the levels of soluble fragments of APP, especially sAPPβ, the product of BACE1, as well as the levels of BACE1 mRNA and the expression of the protein itself increased after 15 minutes of global ischemia in rats and returned to control values after 120 minutes of reperfusion [42], and in our case, we examined the protein level only 4 hours after ischemia. On the other hand, it is known that, in addition to APP, BACE1 substrates are other transmembrane proteins, such as: membrane-bound α2,6-sialyltransferase localized in the Golgi, P-selectin glycoprotein ligand-1 (PSLG-1), APP homologous proteins APLP1 and APLP2, protein , associated with the low density lipoprotein receptor (LRP), voltage-gated sodium channel (Nav1), β2 subunit (Navβ2), neuregulin-1 (NRG1) and neuregulin-3 (NRG3) [43]. Inhibition of BACE1 cleavage of neuregulin-1 (NRG1) and possibly neuregulin-3 (NRG3) causes a decrease in the thickness of the myelin sheath of axons of both peripheral nerves (sciatic nerve) and central optic nerves and impairs remyelination of injured nerves [44].

 doi:10.20944/preprints202205.0184.v1

Also, proteolytic processing of the neuregulin-1 (NRG1) BACE1 protein is associated with the activation of ErbB receptor tyrosine kinases. This signaling pathway is involved in synapse formation, plasticity, neuronal migration, myelination of central and peripheral axons, and in the regulation of neurotransmitter expression and function. It is possible that the 7 days after neurotrauma time point that we studied was insufficient to activate the expression of the enzyme, since the available data indicate that high BACE-1 activity in neurons may be associated with repair processes after damage to brain cells.

γ-secretase catalyzes the final cleavage of APP with AICD and either Aβ in the case of the amyloidogenic pathway of APP proteolysis or p3 in the non-amyloidogenic variant of APP proteolytic formation (Fig. 1). γ-secretase is composed of four integral membrane proteins, presenilin (PS) 1 or 2, nicastrin (NCT), PEN-2, and APH-1. Assembly of the complex begins with the stabilization of PS with nicastrin and APH-1, after which the last component of the PEN-2 protein complex is added [45]. Biochemical studies show that PS1 and PS2 (or APH-1a and APH-1b and their alternatively spliced forms) never coexist in the same complex, suggesting that there are at least six different γ-secretase complexes in humans. It was found that PS1 is located mainly in the endoplasmic reticulum [46]. However, significant amounts of PS1 bound to NCT were found in the plasma membrane, in endosomes/lysosomes, indicating that the fully assembled complexes leave the endoplasmic reticulum and translocate to the plasma membrane. Subsequently, all four components of the γ-secretase complex are localized in the active form on the plasma membrane and in lysosomes [46]. Our studies have shown that the expression of proteins of the γ-secretase complex: PS1 and nicastrin increases in astrocytes, but not in penumbra neurons on the first day after PTS and remains high up to 7 days after PTS. However, it was shown that after global ischemia, PS1 expression decreased from 2 up to 7 days, but the trend was reversed on day 30 [47].

There is no data on the role of another component of the γ-secretase complex, nicastrin, in the development of damage during ischemia. We carried out an inhibitory analysis in order to understand the significance of the detected changes in the expression of α-, β-, and γ-secretase proteins.

Batimastat or BB-94 was used as an α-secretase inhibitor. The inhibitor molecule mimics the metalloproteinase substrate and therefore acts by competitive reversible inhibition [26]. In a number of studies, BB-94 is used to study APP processing [27] and the role of its proteolytic products in memory processes and the pathogenesis of Alzheimer's disease [28]. Batimastat is almost completely insoluble and therefore has very low oral bioavailability. Thus, the only way to administer batimastat is by direct injection into various body cavities (abdominal and pleural) [26]. It has been previously demonstrated that BB-94 efficiently enters the brain when administered intraperitoneally [21, 32]. The dose we chose (50 mg/kg) of BB-94 was shown to have a neuroprotective effect in a mouse model of focal cerebral ischemia[21, 23]. A number of studies have demonstrated the neuroprotective effect of an inhibitor with a decrease in infarct volume [21], an improvement in neurological functions, and a decrease in mortality in various models of ischemic stroke in rats and mice [48-50], as well as excitotoxic damage to neurons in cell culture [51]. However, we failed to detect the effect of the drug on changes in infarct volume or the level of apoptosis of mouse cerebral cortex cells.

LY2886721 is a potent and selective active site inhibitor of β-secretase (BACE1,2) without inhibition of other proteases such as cathepsin D, pepsin and renin [22, 33]. LY2886721 demonstrates an effective dose-dependent decrease in the level of Aβ and sAPPβ in a different experimental models: in HEK293 cells with the APP751 mutation; in primary cortical neurons of PDAPP-mutated mice [52] ; in vivo animal models (3-30 mg/kg PDAPP mice, 1.5 mg/kg beagle dogs; orally) [22, 52-54]. In transgenic mice, doses of 3–30 mg/kg reduced Aβ levels by 20–65%. The effect lasted up to nine hours after application of the drug. A decrease in amyloid production has been observed in plasma and cerebrospinal fluid after administration of LY2886721 [22, 33]. In a beagle dog model, oral administration (1.5 mg/kg) showed a significant and persistent reduction in Aβ levels

 doi:10.20944/preprints202205.0184.v1

in the cerebrospinal fluid [54]. However, as in the case of batimastat, we failed to detect the effect of LY2886721 on changes in infarct volume or the level of apoptosis of mouse cerebral cortex cells after ischemic stroke.

DAPT (N-[N- (3,5-difluorophenacetyl)-1-alanyl]-Sphenylglycine t-butylester) is a γ-secretase inhibitor. Of the three secretase inhibitors studied, only DAPT reduced the infarct volume on days 7 and 14 after PTS, preventing the growth of apoptosis of mouse cerebral cortex cells in the area adjacent to the infarction zone. It is known from the literature that this inhibitor was used to treat neurodegenerative diseases and modulated the differentiation of progenitor neurons and apoptotic cascades in neurons during cerebral ischemia [23]. DAPT protects the brain from cerebral ischemia [55] by influencing inflammatory processes, in particular by suppressing the expression of NF-κB, a family of transcription factors involved in ischemic injury and promoting inflammatory processes, by inducing neuronal apoptosis [56-57]. DAPT has been shown to have a pronounced neuroprotective effect in a mouse model of ischemia/reperfusion (I/R) caused by occlusion of the middle cerebral artery. DAPT significantly improved neurobehavioral performance and reduced neuronal morphological damage. In addition, DAPT reduced the level of GFAP as well as the number of apoptotic cells by reducing the content of interleukin-6 and tumor necrosis factor-α [58]. In this work, we also showed that photothrombotic stroke causes an increase in the level of γ-secretase proteins PS1 and nicastrin mainly in astrocytes, and the administration of the inhibitor reduced the level of GFAP. Probably, inhibition of γ-secretase enhances the anti-inflammatory response and reduces the activation of astrocytes, which contributes to a decrease in the level of apoptosis and, as a consequence, the amount of damage after ischemia. Thus, DAPT can be considered as a drug for stroke therapy.

5. Conclusion and further perspectives

The processing of APP is involved in the pathogenesis of many neurodegenerative disorders. We have investigated the expression of APP and its processing proteases such as α-secretase of ADAM10, β-secretase of BACE1, γ-secretase subunits of PS1 and NCT in a PTS mice model by using immunoblotting, electron immunohistochemistry and immunofluorescence. The results showed that the accumulation of APP in the cytoplasm of the neuron was increased at 24 hours after PTS with significant tissue damage, lysis of nuclei, destruction of cells. Furthermore, α-secretase of ADAM10 was proven to be mainly present in the cytoplasmic fraction of the penumbral tissue and was increased significantly in neurons at 24 hours after PTS. However, no significant difference was found in different times after PTS for the expression of β-secretase of BACE1 although the expression of BACE1 in neurons and astrocytes of the rat cerebral cortex seemed relatively low. Interestingly, both γ-secretase subunits of PS1 and NCT were shown to increase in astrocytes at 24 hours after PTS. To further discover the roles of these secretases, Batimastat (BB-94), an α-secretase inhibitor, LY2886721, a β-secretase inhibitor and DAPT, a γ-secretase inhibitor, were used in a PTS mice model. Among these, only DAPT can reduce the infarct volume on days 7 and 14 after PTS, preventing the growth of mouse cerebral cortex cell apoptosis in the area adjacent to the infarction zone. Regarding the positive correlation of the expression of APP, α-secretase of ADAM10 and γ-secretase subunits of PS1 and NCT after PTS, further research to reveal the exact roles of these proteins in stroke would be interesting and valuable to explore.

In conclusion, we demonstrated that a photothrombotic stroke led to reduced the expression of ADAM10 α-secretase in neurons and increased the levels of the γ-secretase subunits of PS1 and NCT in astrocytes. Furthermore, the inhibitory assay showed that only the γ-secretase inhibitor of DAPT reduces GFAP levels and decreases brain infarct volume, suggesting γ-secretase appear to be a therapeutic target and its inhibitor of DAPT may have the therapeutic potential for the treatment of stroke.

 doi:10.20944/preprints202205.0184.v1

Funding: This work was funded by the grant of the Ministry of Science and Higher Education of the Russian Federation, No. 0852-2020-0028 and Guizhou Science and Technology Department of China (no. ZK[2022]035).

Author Contributions: Conceptualization, Svetlana Sharifulina and Svetlana Demyanenko; Data curation, Svetlana Sharifulina and Svetlana Demyanenko; Formal analysis, Svetlana Sharifulina, Valeria Guzenko, Alexandr Logvinov, Yuliya Kalyuzhnaya, Natalia Dobaeva, Yan Li and Lei Chen; Funding acquisition, Bin He and Svetlana Demyanenko; Investigation, Svetlana Sharifulina, Valeria Guzenko, Alexandr Logvinov, Andrey Khaitin, Yuliya Kalyuzhnaya, Natalia Dobaeva, Yan Li, Lei Chen, Bin He and Svetlana Demyanenko; Methodology, Svetlana Sharifulina, Valeria Guzenko, Alexandr Logvinov, Yuliya Kalyuzhnaya, Yan Li, Lei Chen and Svetlana Demyanenko; Project administration, Svetlana Sharifulina and Svetlana Demyanenko; Resources, Svetlana Sharifulina; Software, Svetlana Sharifulina, Andrey Khaitin, Yuliya Kalyuzhnaya, Yan Li and Svetlana Demyanenko; Supervision, Svetlana Sharifulina and Svetlana Demyanenko; Validation, Svetlana Sharifulina, Valeria Guzenko, Alexandr Logvinov, Andrey Khaitin, Yuliya Kalyuzhnaya, Natalia Dobaeva, Yan Li and Bin He; Visualization, Svetlana Sharifulina, Yuliya Kalyuzhnaya and Natalia Dobaeva; Writing – original draft, Svetlana Sharifulina and Svetlana Demyanenko; Writing – review & editing, Svetlana Sharifulina, Bin He and Svetlana Demyanenko. All authors have read and agreed to the published version of the manuscript.

Institutional Review Board Statement: The study was conducted according to the guidelines of the Declaration of Helsinki, and approved by the Animal Care and Use Committee of the Southern Federal University (Approval No. 08/2016). Our study did not involve any human subjects.

Informed Consent Statement: Not applicable.

Data Availability Statement: Data is available on demand to corresponding author Dr. Sharifulina

Conflicts of Interest: The authors declare no conflicts of interest.

Supplementary

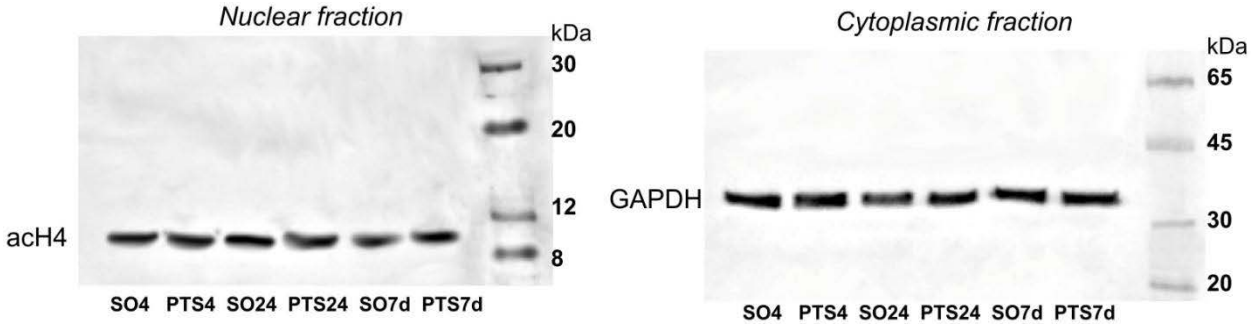

Figure S1. An example of Western blot evaluation of the purity of the obtained nuclear and cytoplasmic fractions of the cerebral cortex of sham-operated rats, penumbra tissue after 4 (PTS4h), 24 (PTS24h) hours and 7 days (PTS7d) after photothrombotic stroke (PTS) in rats. The acetylated histone H4 protein (ac-H4) was used as a nuclear fraction marker. Anti-acetyl-Histone H4 produced in rabbit (#06-866, Merck) diluted 1:500 was used. The protein glyceraldehyde-3-phosphate dehydrogenase (GAPDH) was used as a marker of the cytoplasmic fraction. Anti-GAPDH antibody produced in rabbit (G9545, Sigma-Aldrich) diluted 1:1000 was used.

References

1. Orellana-Urzúa, S.; Rojas, I; Líbano, L; Rodrigo, R. Pathophysiology of Ischemic Stroke: Role of Oxidative Stress. Curr. Pharm. Des. 2020, 26, 4246-4260. doi: 10.2174/1381612826666200708133912.

2. Iadecola, C.; Anrather, J. Stroke research at a crossroad: asking the brain for directions. Nat. Neurosci. 2011, 14, 1363–1368. doi: 10.1038/nn.2953.
3. Hankey G.J. Stroke. Lancet 2017, 389, 641–654. doi: 10.1016/S0140-6736(16)30962-X.
4. Demyanenko, S; Uzdensky, A. Profiling of Signaling Proteins in Penumbra After Focal Photothrombotic Infarct in the Rat Brain Cortex. Mol. Neurobiol. 2017, 54, 6839-6856. doi: 10.1007/s12035-016-0191-x.
5. Jacobsen, K.T.; Iverfeldt, K. Amyloid precursor protein and its homologues: a family of proteolysis-dependent receptors. Cell. Mol. Life Sci. 2009, 66, 2299-22318. doi: 10.1007/s00018-009-0020-8.
6. Guo, Q; Wang, Z.; et al. APP physiological and pathophysiological functions: insights from animal models. Cell Res. 2012, 22, 78-89. doi: 10.1038/cr.2011.116.
7. Dawkins, E.; Small, D.H. Insights into the physiological function of the β-amyloid precursor protein: beyond Alzheimer's disease. J. Neurochem. 2014, 129, 756-769. doi: 10.1111/jnc.12675.
8. Müller, U.C.; Deller, T.; Korte, M. Not just amyloid: physiological functions of the amyloid precursor protein family. Nat. Rev. Neurosci. 2017, 18, p.281-298. doi: 10.1038/nrn.2017.29.
9. Hefter, D.; Draguhn, A. APP as a Protective Factor in Acute Neuronal Insults. Front. Mol. Neurosci. 2017, 10, 22. doi:10.3389/fnmol.2017.00022
10. Pluta, R.; Ułamek-Kozioł, M.; Januszewski, S.; Czuczwar, S.J. Participation of Amyloid and Tau Protein in Neuronal Death and Neurodegeneration after Brain Ischemia. Int. J. Mol. Sci. 2020, 21, 4599. doi: 10.3390/ijms21134599.
11. Haass, C.; Kaether, C.; et al. Trafficking and Proteolytic Processing of APP. Cold Spring Harb. Perspect. Med. 2012, 2, a006270–a006270. doi:10.1101/cshperspect.a006270
12. Vincent, B.; Govitrapong, P. Activation of the α-secretase processing of AβPP as a therapeutic approach in Alzheimer's disease. J. Alzheimers Dis. 2011, 24, p.75-94. doi: 10.3233/JAD-2011-110218.
13. Vincent, B. Regulation of the α-secretase ADAM10 at transcriptional, translational and post-translational levels. Brain Res. Bull. 2016, 126, 154-169. doi: 10.1016/j.brainresbull.2016.03.020.
14. Endres, K.; Deller, T. Regulation of Alpha-Secretase ADAM10 In vitro and In vivo: Genetic, Epigenetic, and Protein-Based Mechanisms. Front. Mol. Neurosci. 2017, 10. doi: 10.3389/fnmol.2017.00056
15. Zhang, X.; Zhou, K.; Wang, R.; et al. Hypoxia-inducible factor 1alpha (HIF-1alpha)-mediated hypoxia increases BACE1 expression and beta-amyloid generation. J. Biol. Chem. 2007, 282, 10873-10881. doi: 10.1074/jbc.M608856200.
16. Guglielmotto, M.; Aragno, M.; Autelli, R.; et al. The up-regulation of BACE1 mediated by hypoxia and ischemic injury: role of oxidative stress and HIF1alpha. J. Neurochem. 2009, 108, 1045-1056. doi: 10.1111/j.1471-4159.2008.05858.x.
17. Carroll, C.M.; Li, Y.M. Physiological and pathological roles of the γ-secretase complex. Brain Res. Bull. 2016, 126, 199-206. doi: 10.1016/j.brainresbull.2016.04.019.
18. Uzdensky, A.B. Photothrombotic Stroke as a Model of Ischemic Stroke. Transl. Stroke Res. 2018, 9, 437-451. doi: 10.1007/s12975-017-0593-8.
19. Demyanenko, S.; Uzdensky, A. Profiling of Signaling Proteins in Penumbra After Focal Photothrombotic Infarct in the Rat Brain Cortex. Mol. Neurobiol. 2016, 54, 6839–6856. doi:10.1007/s12035-016-0191-x.
20. Uzdensky, A.; Demyanenko, S.; et al. Photothrombotic infarct in the rat brain cortex: Protein profile and morphological changes in penumbra. Mol. Neurobiol. 2017, 54, 4172–4188. doi: 10.1007/s12035-016-9964-5.
21. Asahi, M.; Asahi, K.; et al. Role for matrix metalloproteinase 9 after focal cerebral ischemia: effects of gene knockout and enzyme inhibition with BB-94. J. Cereb. Blood Flow Metab. 2000, 20, 1681–1689. doi: 10.1097/00004647-200012000-00007
22. May, P. C.; Willis, B. A.; et al. The potent BACE1 inhibitor LY2886721 elicits robust central Aβ pharmacodynamic responses in mice, dogs, and humans. J. Neurosci. 2015, 35, 1199–1210. doi: 10.1523/JNEUROSCI.4129-14.2015
23. Zhang, G. S.; Tian, Y.; et al. The γ-secretase blocker DAPT reduces the permeability of the blood-brain barrier by decreasing the ubiquitination and degradation of occludin during permanent brain ischemia. CNS Neurosci. Ther. 2013, 19, 53–60. doi: 10.1111/cns.12032
24. Musi, C. A.; Agrò, G.; et al. JNK3 as Therapeutic Target and Biomarker in Neurodegenerative and Neurodevelopmental Brain Diseases. Cells 2020, 9, 2190. doi: 10.3390/cells9102190
25. Cai, Z.; Liu, Z.; et al. Chronic Cerebral Hypoperfusion Promotes Amyloid-Beta Pathogenesis via Activating β/γ-Secretases. Neurochem. Res. 2017, 42, 3446-3455. doi:10.1007/s11064-017-2391-9
26. Rasmussen, H. S.; McCann, P. P. Matrix metalloproteinase inhibition as a novel anticancer strategy: a review with special focus on batimastat and marimastat. Pharmacol. Ther. 1997, 75, 69–75. doi: 10.1016/s0163-7258(97)00023-5
27. Paschkowsky, S.; Hamzé, M.; et al. Alternative Processing of the Amyloid Precursor Protein Family by Rhomboid Protease RHBDL4. J. Biol. Chem. 2016, 291, 21903–21912. doi: 10.1074/jbc.M116.753582
28. Dubrovskaya, N. M.; Nalivaeva, N. N.; et al. Effects of an inhibitor of alpha-secretase, which metabolizes the amyloid peptide precursor, on memory formation in rats. Neurosci. Behave. Physiol. 2006, 36, 911–913. doi: 10.1007/s11055-006-0106-9
29. Goss, K. J.; Brown, P. D.; Matrisian, L. M. Differing effects of endogenous and synthetic inhibitors of metalloproteinases on intestinal tumorigenesis. Int. J. Cancer 1998, 78, 629–635. doi: 10.1002/(sici)1097-0215(19981123)78:5<629::aid-ijc17>3.0.co;2-8
30. Knecht, T.; Story, J.; et al. Adjunctive Therapy Approaches for Ischemic Stroke: Innovations to Expand Time Window of Treatment. Int. J. Mol. Sci. 2017, 18, 2756. doi: 10.3390/ijms18122756
31. Sumii, T.; Lo, E. H. Involvement of matrix metalloproteinase in thrombolysis-associated hemorrhagic transformation after embolic focal ischemia in rats. Stroke 2002, 33, 831–836. doi: 10.1161/hs0302.104542

32. Páez Pereda, M.; Ledda, M. F.; et al. High levels of matrix metalloproteinases regulate proliferation and hormone secretion in pituitary cells. J. Clin. Endocrinol. Metab. 2000, 85, 263–269. doi: 10.1210/jcem.85.1.6248
33. Miranda, A.; Montiel, E.; et al. Selective Secretase Targeting for Alzheimer's Disease Therapy. J. Alzheimer's Dis. 2021, 81, 1–17. doi: 10.3233/JAD-201027
34. Zhang, Y.; Xiang, Z.; et al. The Notch signaling pathway inhibitor Dapt alleviates autism-like behavior, autophagy and dendritic spine density abnormalities in a valproic acid-induced animal model of autism. Prog. Neuropsychopharmacol. Boil. Psychiatry 2019, 94, 109644. doi: 10.1016/j.pnpbp.2019.109644
35. Koike, M. A.; Lin, A. J.; et al. APP Knockout Mice Experience Acute Mortality as the Result of Ischemia. PLoS ONE 2012, 7, e42665. doi:10.1371/journal.pone.0042665
36. Saftig, P.; Lichtenthaler, S.F. The alpha secretase ADAM10: A metalloprotease with multiple functions in the brain. Prog. Neurobiol. 2015, 135, 1-20. doi:10.1016/j.pneurobio.2015.10.003.
37. El Bejjani, R.; Hammarlund, M. Notch Signaling Inhibits Axon Regeneration. Neuron 2012, 73, 268–278. doi:10.1016/j.neuron.2011.11.017
38. Warren, K. M.; Reeves, T. M.; Phillips, L. L. MT5-MMP, ADAM-10, and N-Cadherin Act in Concert To Facilitate Synapse Reorganization after Traumatic Brain Injury. J. Neurotrauma 2012, 29, 1922–1940. doi:10.1089/neu.2012.2383
39. Lee, P. H.; Hwang, E. M.; et al. Effect of Ischemic Neuronal Insults on Amyloid Precursor Protein Processing. Neurochem. Res. 2006, 31, 821–827. doi:10.1007/s11064-006-9086-y
40. Horste, G. M. zu; Derksen, A.; et al. Neuronal ADAM10 Promotes Outgrowth of Small-Caliber Myelinated Axons in the Peripheral Nervous System. J. Neuropathol. Exp. Neurol. 2015, 74, 1077–1085. doi:10.1097/nen.0000000000000253
41. Thonda, S.; Puttapaka, S.N.; et al. Extracellular-Signal-Regulated Kinase Inhibition Switches APP Processing from β- to α-Secretase under Oxidative Stress: Modulation of ADAM10 by SIRT1/NF-κB Signaling. ACS Chem. Neurosci. 2021, 12, 4175-4186. doi:10.1021/acschemneuro.1c00582
42. Babusikova, E.; Dobrota, D.; et al. Effect of Global Brain Ischemia on Amyloid Precursor Protein Metabolism and Expression of Amyloid-Degrading Enzymes in Rat Cortex: Role in Pathogenesis of Alzheimer's Disease. Biochemistry 2021, 86, 680–692. doi:10.1134/S0006297921060067
43. Vassar, R.; Kovacs, D. M.; et al. The β-Secretase Enzyme BACE in Health and Alzheimer's Disease: Regulation, Cell Biology, Function, and Therapeutic Potential.J. Neurosci. 2009, 29, 12787–12794. doi:10.1523/jneurosci.3657-09.2009
44. Hu, X.; He, W.; et al. Genetic deletion of BACE1 in mice affects remyelination of sciatic nerves. FASEB J. 2008, 22, 2970-2980. doi:10.1096/fj.08-106666
45. Kaether, C.; Haass, C.; Steiner, H. Assembly, Trafficking and Function of γ-Secretase. Neurodegener. Dis. 2006, 3, 275–283. doi:10.1159/000095267
46. Tolia, A.; De Strooper, B. Structure and function of γ-secretase. Semin. Cell Dev. Biol. 2009, 20, 211–218. doi:10.1016/j.semcdb.2008.10.007
47. Pluta, R.; Kocki, J.; et al. Alzheimer-associated presenilin 2 gene is dysregulated in rat medial temporal lobe cortex after complete brain ischemia due to cardiac arrest. Pharmacol. Rep. 2016, 68, 155–161. doi:10.1016/j.pharep.2015.08.002
48. Knecht, T.; Borlongan, C.; Dela Peña, I. Combination therapy for ischemic stroke: Novel approaches to lengthen therapeutic window of tissue plasminogen activator. Brain circ. 2018, 4, 99–108. doi: 10.4103/bc.bc_21_18
49. Walz, W.; Cayabyab, F.S. Нейтрофильная инфильтрация и матричная металлопротеиназа-9 при лакунарном инфаркте. Neurochem. Res. 2017, 42, 2560–2565. doi: 10.1007/s11064-017-2265-1
50. Lapchak, P. A.; Chapman, D. F.; Zivin, J. A. Metalloproteinase inhibition reduces thrombolytic (tissue plasminogen activator)-induced hemorrhage after thromboembolic stroke. Stroke 2000, 31, 3034–3040. doi: 10.1161/01.str.31.12.3034
51. Chapman, G. A.; Moores, K.; et al. Fractalkine cleavage from neuronal membranes represents an acute event in the inflammatory response to excitotoxic brain damage. J. Neurosci. 2000, 20, RC87. doi: 10.1523/JNEUROSCI.20-15-j0004.2000
52. Dekeryte, R.; Franklin, Z.; et al. The BACE1 inhibitor LY2886721 improves diabetic phenotypes of BACE1 knock-in mice. Biochim. Biophys. Acta Mol. Basis Dis. 2021, 1867, 166149. doi: 10.1016/j.bbadis.2021.166149
53. Satir, T. M.; Agholme, L.; et al. Partial reduction of amyloid β production by β-secretase inhibitors does not decrease synaptic transmission. Alzheimer's Res. Ther. 2020, 12, 63. doi: 10.1186/s13195-020-00635-0
54. Kumar, D.; Ganeshpurkar, A.; et al. Secretase inhibitors for the treatment of Alzheimer's disease: Long road ahead. Eur. J. Med. Chem. 2018, 148, 436–452. doi: 10.1016/j.ejmech.2018.02.035
55. Jin, Z.; Guo, P.; et al. Neuroprotective effects of irisin against cerebral ischemia/ reperfusion injury via Notch signaling pathway. Biomed. pharmacother. 2019, 120, 109452. doi: 10.1016/j.biopha.2019.109452
56. Li, S.; Zyang, X.; et al. DAPT protects brain against cerebral ischemia by down-regulating the expression of Notch 1 and nuclear factor κB in rats. Neurol. Sci. 2012, 33, 1257–1264. doi: 10.1007/s10072-012-0948-6
57. Li, Z.; Wang, J.; et al. Acute Blockage of Notch Signaling by DAPT Induces Neuroprotection and Neurogenesis in the Neonatal Rat Brain After Stroke. Transl. stroke Res. 2016, 7, 132–140. doi: 10.1007/s12975-015-0441-7
58. Wang, J.J.; Zhu, J.D.; et al. Neuroprotective effect of Notch pathway inhibitor DAPT against focal cerebral ischemia/reperfusion 3 hours before model establishment. Neural. Regen. Res. 2019, 14, 452-461. doi:10.4103/1673-5374.245469